

Contents lists available at ScienceDirect

Chemical Geology

journal homepage: www.elsevier.com/locate/chemgeo



Geochemical composition of Aeolian dust and surface deposits from the Qatar Peninsula



Oguz Yigiterhan^{a,*}, Balint Z. Alfoldy^a, Mariasilvia Giamberini^b, Jesse C. Turner^c, Ebrahim S. Al-Ansari^a, Mohamed A. Abdel-Moati^d, Ibrahim A. Al-Maslamani^a, Mohamed M. Kotb^a, Elnaiem A. Elobaid^a, Hassan M. Hassan^a, Jeffrey P. Obbard^a, James W. Murray^c

- ^a Qatar University, Environmental Science Center, P.O. Box 2713, Qatar
- ^b Istituto di Geoscienze e Georisorse, Consiglio Nazionale delle Ricerche, Via Moruzzi, 1 56124, Pisa, Italy
- ^c University of Washington, School of Oceanography, Box 355351, Seattle, WA 98195-5351, USA
- d Ministry of the Environment, Environmental Assessment Department, P.O. Box 39320, Qatar

ARTICLE INFO

Editor: K Johannesson Keywords: Aeolian dust Road traffic dust Atmospheric deposition Dust composition Terrestrial deposits Continental crust Major elements Trace elements Trace metals Enrichment factors Dust collection Passive dust trap Qatar geochemistry Arabian Gulf

Arabian Peninsula

ABSTRACT

The trace metal geochemistry of atmospheric dust and terrestrial surface particles were studied on the Qatar Peninsula from February 2014 to November 2015. We included samples of the mega dust-storm event on 01-02 April 2015. Atmospheric dust samples were collected using passive dust traps. Terrestrial surface deposits of recent dust accumulation and traffic particulate from roads were also sampled. All samples were total acid digested and analyzed for major and trace elements using ICP-OES analyzer. The concentration of thirteen elements (Ca, Mg, Ag, As, Cd, Cr, Cu, Mo, Ni, Se, Sn, Sr, Zn) were enriched in atmospheric dust samples, relative to upper continental crust (UCC). Calcium was especially enriched by up to 435% relative to UCC. About 33% of the total sample mass was CaCO₃, reflecting the composition of surface rocks and soils in the source areas. Of the elements typically associated with anthropogenic activity, Ag, Ni, and Zn were most enriched relative to UCC, with enrichment factors (EF) of 182%, 233%, and 209%, respectively. Other metals, which normally reflect anthropogenic sources, including Pb and V, were not significantly enriched, with enrichment factors of 25% and 3%, respectively. Major elements (Al, Mn, Fe) were depleted (-58%, -35%, and -5%, respectively) relative to UCC due to the large dilution effect of the enrichment of CaCO3. Back trajectories were determined at the date of sampling for each sample using the NOAA HYSPLIT model. These showed that the source of the dust particles was almost equally divided between northerly and southerly sources, except one sample, which appeared to originate from the west. More variability in particle source locations were observed during the winter months (October to March). Samples from the mega-dust storm were solubilized using an acetic acid-hydroxylamine hydrochloride leach procedure to obtain an upper estimate of the potential contribution of bioactive elements to surface seawater. The leach procedure solubilized a significant fraction of almost all elements. Ca was the element most affected (81% removed) because of the carbonate minerals present. Bioactive elements like Fe (25%) and P (58%) were also significantly solubilized. Because river input is so small to the Arabian Gulf, this solubilized fraction of dust is likely a major source of nutrients to surface seawater. Enrichment factors were also calculated with respect to the average composition of terrestrial surface deposits (TSD). Samples are not enriched significantly with respect to major components (EF < 2), with a depletion in Ca, K, Na in dust storm samples, reflecting a different origin. A significant enrichment of the same trace metals is evident in dust deposits and in traffic samples, but not in dust storms: Cu, Mo, Ni, Zn, possibly deriving from local atmospheric sources (traffic, industries). Samples with northern and southern origins were compared to see if the composition could be used to identify source. Only three elements were observed to be statistically different. Pb and Na were higher in samples from the south, while Cr was higher in those from the north.

^{*} Corresponding author at: Qatar University, Environmental Science Center, Marine Sciences Cluster, P.O. Box: 2713, Doha, Qatar E-mail address: oguz@qu.edu.qa (O. Yigiterhan).

1. Introduction

The deserts of the Earth are huge sources of dust (e.g., Prospero, 1996). North Africa and the Middle East supply one half of the global dust burden. It is well established that Aeolian transport (dust lifted by weather) is an important pathway for delivering lithogenic material from the continents to the oceans, and marginal seas (e.g., Blank et al., 1985; Guieu et al., 2010; Buck et al., 2013). Such land derived materials account for a large portion of marine sediments (Windom, 1975). Dusts from different sources often have different chemical compositions on a regional scale and the compositions can be used to aid in the identification of the source (Scheuvens et al., 2013). In some cases, the composition indicates anthropogenic contamination (e.g. Chen et al., 2008; Ranville et al., 2010; Patey et al., 2015).

Atmospheric dust is a major source of bioavailable Fe to the oceans (Jickells et al., 2005; Moore and Braucher, 2008). Its variability over time plays a significant role in influencing the temporal variability of global food-web structure, primary productivity, and other biogeochemical cycles (Martin et al., 1994; McGee et al., 2007; Sur et al., 2015). Selective leaching techniques (e.g., Berger et al., 2008; Rauchenberg and Twining, 2015) have been used to identify the fraction of iron and other elements that may be soluble and possibly bioreactive when atmospheric dust enters seawater (Hanson et al., 2001). Models have been used to simulate the sources, transport, and deposition of atmospheric particles to the ocean (e.g., Fung et al., 2000; Aumont et al., 2008; Wang et al., 2015).

The composition of dust deposited in the Arabian Gulf and Arabian Sea is influenced by seasonal and anthropogenic factors. Overall, the greatest influx of dust occurs during winter and spring, and the compositions of dust can vary between seasons (Pease et al., 1998). Anthropogenic enrichments of Zn, Cd, and Pb have been observed in dust in the Arabian Sea. These metals typically occur at higher concentrations during the northeast (NE) monsoon i.e. March, than during the inter-monsoon month i.e. May, or the southwest (SW) monsoon months of July and August (Johansen and Hoffmann, 2003). These elements were also found to be highly enriched compared to average crust concentrations in "unpolluted" marine sediments in Kuwait (Samhan et al., 1986), thereby indicating the influence that pollution and urban areas may have on the input of trace metals to the Arabian Sea. Siefert et al. (1999) found that many metal concentrations (Al, Fe, Mn, V, Pb, Mo, Cr, Cu) were higher during the inter-monsoon season, when air masses originate over landmasses, indicating both a natural crustal influence (possibly ultramafic rock) and anthropogenic influence. Seasonal variation was also observed in samples from Riyadh, Saudi Arabia (Modiahsh, 1997). Alghamdi et al. (2015) concluded that S, Cl, Co, Cu, Zn, Ga, As, Pb, Cd, V, and Ni all had anthropogenic sources in Jeddah, Saudi Arabia. Na concentrations in aerosols/dust increased during the southwest monsoon, indicative of sea-salt contributions (Siefert et al.,

The Arabian Peninsula is one of the largest desert areas in the world, with physical and geographical features characterized by hyper arid conditions. In the winter and spring there can be winds from the SE (Kaus winds). In the summer months dry winds from the NW (Shamal winds) predominate (Al-Sanad et al., 1993). Rainstorms occur in the region from December to April and these can occasionally be quite strong. Dust storms are common throughout the year, but especially during the period of NW winds. These hot, dry, dusty, Shamal winds from Iraq and the Arabian Gulf states (including Saudi Arabia and Kuwait), blow almost continuously, but decrease at night, and cause great dust storms (El-Baz and Makharita, 2009). On average, there are about 13 dust storm events per year with 77% in the summer (Al-Senafi and Anis, 2015). The nature and direction of the transported dust particles to Qatar Peninsula during these events vary depending on wind strength, altitute, and direction (Fig. 1a, b). There has been an increase in dust after the Gulf War (1990-1991) and Operation Iragi Freedom (2003) (Al-Senafi and Anis, 2015).

The State of Qatar occupies a small, flat, limestone peninsula, which stretches north from the Saudi Arabian Peninsula into the Arabian/ Persian/Basra Gulf (Fig. 2). Geological and structural maps of Qatar can be found in ESC (2014). The surficial geology is characterized by its gentle slope and dominated by Eocene carbonate deposits. Qatar has two very large sabkha (Dukhan and Umm Said) with huge gypsum mineral deposits. The main structural feature is a broad anticline along the axis of the peninsula. Its highest point is only about 100 m above mean sea level. Therefore, the distribution and deposition of the surface sediments is mainly controlled by wind action, namely the prevailing Shamal (North) wind, which blows from the northwest (NW) or northnorthwest (NNW). The superficial Aeolian sands, of Holocene age, cover large areas of Oatar Peninsula and neighboring countries, and are considered as the most common surface feature, distributed irregularly in the form of mobile thin sheets of sand, and sand dunes. The Qatari Aeolian sands are classified as silico-calcareous type and concentrated in the southern part, and along the southeastern corner and the northeastern coastal zone of the country (Cavelier, 1970). Sand dunes begin about half way down the peninsula. These occur first as relatively small, scattered dunes which agglomerate, then become larger, as they migrate south (S) /southeast (SE) towards Saudi Arabia and meet the sea at the southeast corner of Qatar in Fig. 2. The movement of sand is driven down the peninsula by the northwesterly Shamal winds which transport the sand dunes by around eleven meters. The expansive deserts on the Arabian Peninsula and Kuwait and the dry Mesopotamian flood plain deposits in Iraq (Khalaf et al., 1985) provide key dust storm ingredients such as limited precipitation, scarce vegetation, ample dust and sand sources as well as unstable, thermally mixed air providing essential vertical transport.

This is the first comprehensive study of the composition of atmospheric dust and source materials in this region. Samples of atmospheric dust and local terrestrial surficial deposits were collected from different land based sites on the Qatar Peninsula. This is important because the atmospheric dust is the main source of terrigenous material deposited to sediments in the adjacent Arabian Gulf (Al-Naimi et al., 2015). In the water column, trace elements, like iron (Fe), from these materials can influence marine biological food-web structure as well as marine biological productivity. The main sources of suspended matter in the Arabian Gulf around Qatar are atmospheric dust and plankton (Yigiterhan et al., in submission.). This paper focuses on the chemical composition of the dust end-member. Surficial soil and dust samples can be useful tracers of contamination pathways from air emissions to the sea (El-Sayed et al., 2010).

2. Sampling locations and techniques

This study included samples of atmospheric dust and terrestrial surface samples (recently deposited dust) from selected locations remote from capital city Doha, coastal settlements and major industrial cities (Fig. 2). Atmospheric dust samples are described in Table 1, while surface terrestrial deposits are described in Table 2.

2.1. Atmospheric dust samples

Atmospheric dust was sampled at six locations shown in Fig. 2. Each was carefully selected to reflect differences in the influences of local traffic, construction, industry, or rural residency along the eastern coast of Qatar, where most of the Qatar's population and industry are heavily located.

Al Khor station was located at the north of Doha city, located at the center of east coast. A passive sampler was located close to the fisherman wharf. This is the location of the major traditional fishing fleet in Qatar. Al Tarfa station was located at Qatar University, a fast-growing district, northeast of central Doha. There are numerous construction projects on-going inside and outside the university campus. Heavy equipment was continuously excavating calcareous rocks within 1 km

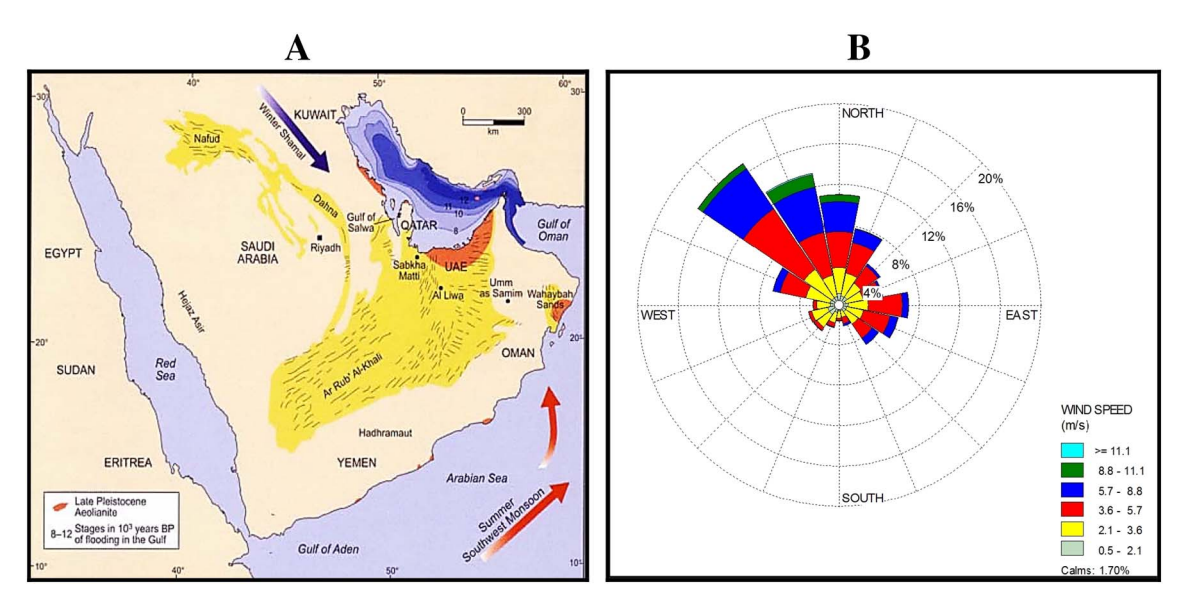


Fig. 1. a. Common wind directions shown as blue and red colored arrows over the Gulf Area and the Arabian Peninsula (on the left, personal communication from Qatar-MME); b. The average dominant wind direction for 2011–2015.

(Source: Doha International Airport and sourced from Trinity Consultants, USA)



Fig. 2. Sample locations of Qatari dust and terrestrial surface deposits located on the map of Greater Doha, Doha Bay, Pearl City, West Bay regions (on the left) and for the Qatar peninsula (on the right). Location of Qatar in the Gulf is given on the top left. The dust sampling locations are shown as rectangular yellow boxes. The surface soil deposits were shown as solid red circles.

of the passive sampler while sampling was conducted. *Katara* station was in the largest culture park of Qatar, located in the West Bay region, north of Doha. *Al Dafna* station was setup as a temporary sampling point, near the coastline, at the center of Qatar's capital, where the influence of human activities are maximized. *Al Waab* was an inland station southeast of Doha, located in a residential compound with restricted access. The station was close to Aspire Park and major road intersections. *Sealine* station was south of Doha, along the coast. Depending on wind direction, the passive dust samples from this trap would reflect either the influence of industrial city Mesaieed or the natural sand dunes of Khor Al-Udeid (Fig. 2).

There is almost no rain in Qatar (~3 in. per year from November to

May) so wet deposition is minor. The dust accumulation is usually extensive, so collecting dust is very straight forward but must be done carefully to avoid contamination. Most individual dust samples were collected over 2 to 4 week intervals; however, when there was a dust storm, sampling intervals were as short as overnight. The sampling was done using passive dust traps (SIAP + MICROS brand). The particles were collected in an acid-cleaned glass bowl, which had automated protection from the rain with a digitally controlled closing-opening system, activated with rain sensors, for both dry and wet deposition. These traps were regularly visited during non-stormy autumn and winter seasons from September to February. Sufficient dry dust particle accumulation (> 1 g dry weight) was achieved after a sampling period

Table 1 Sampling information for dust samples, collected in Qatar.

Sample ID	Sampling	Sampling	Deposition 1	period	Sample	Sampling	Sampling	Wind
(units)	Date:	Site:	From:	То:	Туре:	Method:	Coordinates	Directi
D00	21-Feb-2014	Al-Dafna	21-Nov-13	21-Feb-14	Atmospheric deposition	Bulk collection from an open space	N 25.307746° E51.516321°	NW
D01	28-Jul-2014	Al-Dafna	21-Feb-14	28-Jul-14	Stormy weather deposit	Bulk collection from an open space	N 25.307746° E51.516321°	NNW
D02	05-Nov-2014	Al-Khor	22-Mar-14	05-Nov-14	Atmospheric deposition	Passive accumulation in dust collector	N 25.68598° E051.51525°	NNW
D03	05-Nov-2014	Katara	05-Aug-14	05-Nov-14	Atmospheric deposition	Passive accumulation in dust collector	N 25.35000° E051.52440°	NNE
D04	12-Feb-2015	Al-Khor	05-Nov-14	12-Feb-15	Atmospheric deposition	Bulk collection from an open space	N 25.68598° E051.51525°	NW
D05	18-Mar-2015	Al-Khor	12-Feb-15	18-Mar-15	Atmospheric deposition	Passive accumulation in dust collector	N 25.68598° E051.51525°	NW
D06	18-Mar-2015	Katara	05-Nov-14	18-Mar-15	Atmospheric deposition	Passive accumulation in dust collector	N 25.35000° E051.52440°	NW
D07	18-Mar-2015	Sealine	01-Jan-15	18-Mar-15	Atmospheric deposition	Passive accumulation in dust collector	N 24.86108° E051.51548°	NNW
D08	22-Mar-2014	Al-Khor	22-Dec-13	22-Mar-14	Atmospheric deposition	Bulk collection from an open space	N 25.68598° E051.51525°	NW
D09	26-Mar-2014	Sealine	26-Dec-13	26-Mar-14	Atmospheric deposition	Bulk collection from an open space	N 24.86108° E051.51548°	NW
D10	01-Apr-2015	Al-Tarfa	01-Jan-15	01-Apr-15	Dust storm deposition	Bulk collection from an open space	N 25.38053° E051.49023°	NW &
D11	02-Apr-2015	Al-Dafna	28-Jul-14	02-Apr-15	Dust storm deposition	Bulk collection from an open space	N 25.307746° E51.516321°	NW &
D12	03-Apr-2015	Katara	18-Mar-15	03-Apr-15	Dust storm deposition	Bulk collection from an open space	N 25.35000° E051.52440°	NW &
D13	03-Apr-2015	Al-Waab	01-Apr-15	03-Apr-15	Dust storm deposition	Passive accumulation in dust collector	N 25.26107° N051.46455°	NW &
D14	03-Apr-2015	Al-Waab	01-Apr-15	03-Apr-15	Dust storm deposition	Bulk collection from an open space	N 25.26107° N051.46455°	NW &
D15	21-Apr-2015	Al-Waab	03-Apr-15	21-Apr-15	Stormy weather deposition	Bulk collection from an open space	N 25.26107° N051.46455°	NW
D16	30-Apr-2015	Al-Waab	21-Apr-15	30-Apr-15	Atmospheric deposition	Passive accumulation in dust collector	N 25.26107° N051.46455°	NW
D17	02-May-2015	Al-Khor	18-Mar-15	02-May-15	Atmospheric deposition	Passive accumulation in dust collector	N 25.68598° E051.51525°	NW
D18	02-May-2015	Katara	03-Apr-15	02-May-15	Atmospheric deposition	Passive accumulation in dust collector	N 25.35000° E051.52440°	NW
D19	03-May-2015	Sealine	18-Mar-15	03-May-15	Atmospheric deposition	Passive accumulation in dust collector	N 24.86108° E051.51548°	NW
D20	10-May-2015	Al-Waab	30-Apr-15	10-May-15	Atmospheric deposition	Passive accumulation in dust collector	N 25.26107° N051.46455°	NW
D25	16-Jun-2015	Al-Waab	10-May-15	16-Jun-15	Stormy weather deposition	Bulk collection from an open space	N 25.26107° N051.46455°	E
D26	21-Jun-2015	Al-Khor	02-May-15	21-Jun-15	Atmospheric deposition	Passive accumulation in dust collector	N 25.68598° E051.51525°	NW
D27	22-Jun-2015	Katara	02-May-15	22-Jun-15	Atmospheric deposition	Passive accumulation in dust collector	N 25.35000° E051.52440°	NW
D28	23-Jun-2015	Al-Tarfa	01-Apr-15	23-Jun-15	Atmospheric deposition	Passive accumulation in dust collector	N 25.38053° E051.49023°	N
D29	24-Jun-2015	Al-Waab	16-Jun-15	24-Jun-15	Atmospheric deposition	Passive accumulation in dust collector	N 25.26107° N051.46455°	NW
D30	28-Oct-2015	Al-Waab	24-Jun-15	28-Oct-15	Atmospheric deposition	Passive accumulation in dust collector	N 25.26107° N051.46455°	NW
D31	28-Oct-2015	Al-Tarfa	23-Jun-15	28-Oct-15	Atmospheric deposition	Passive accumulation in dust collector	N 25.38053° E051.49023°	N
D32	30-Oct-2015	Sealine	03-May-15	30-Oct-15	Atmospheric deposition	Passive accumulation in dust collector	N 24.86108° E051.51548°	N
D33	31-Oct-2015	Al Khor	21-Jun-15	31-Oct-15	Atmospheric deposition	Passive accumulation in dust collector	N 25.68598° E051.51525°	N
D34	01-Nov-2015	Katara	22-Jun-15	01-Nov-15	Atmospheric deposition	Passive accumulation in dust collector	N 25.35000° E051.52440°	N
D35	06-Jun-2014	Al-Tarfa	06-Mar-14	06-Jun-14	Atmospheric deposition	Passive accumulation in dust collector	N 25.38053° E051.49023°	NNW
D36	06-Jun-2014	Al-Waab	06-Mar-14	06-Jun-14	Atmospheric deposition	Bulk collection from an open space	N 25.26107° N051.46455°	NNW
RD01	05-Jun-2014	Mobile	27-Apr-14	05-Jun-14	Road dust deposition	Active filtration new engine air filter	Doha city (Qatar Peninsula)	_
RD02	05-Jun-2014	Mobile	27-Apr-14	05-Jun-14	Road dust deposition	Active filtration new cabin air filter	Doha city (Qatar Peninsula)	

 Table 2

 Sampling information for terrestrial surface deposits (long term, dry and wet deposition), collected in Qatar.

Sample ID	Sampling date	Sampling site	Location of deposit	Structure of deposit	Color of deposit	Sampling		
						Coordinates		
T00	03-Jun-2013	Al Galail	Top of single dune	Fine sand	Light gray	24°45′03.810″N 51°04′39.570″E		
T01	28-Mar-2015	Al Galail	Bottom of single dune	Coarse sand	Light gray	24°45′05.760″N 51° 04′35.310″E		
T02	28-Mar-2015	Al Galail	Top valley of single dune	Deposits	Black (metallic)	24°45′05.120″N 51° 04′39.090″E		
T03	28-Mar-2015	Musfer Sinkhole	Surrounding soil of cave	Fine deposit	Very pale brown	25°10′30.610″N 51°12′41.990″E		
T04	28-Mar-2015	Musfer Sinkhole	Ground of cave entrance	Fine deposit	Very pale brown	25°10′30.480″N 51°12′42.170″E		
T05	28-Mar-2015	Musfer Sinkhole	Ground of cave midway	Fine deposit	Very pale brown	25°10′30.560″N 51°12′42.230″E		
T06	28-Mar-2015	Musfer Sinkhole	Ground of cave bottom	Fine deposit	Reddish brown	25°10′30.870″N 51°12′42.100″E		
T07	28-Mar-2015	Musfer Sinkhole	Thick layers in cave wall	Hard layer deposits	Yellowish-pale brown	25°10′30.710″N 51°12′42.270″E		
T08	13-May-2015	Sumaysimah	Surface upper layer	Grainy	Reddish-brown	25°35′32.958″N 51°29′10.053″E		
T09	13-May-2015	Sumaysimah	Surface upper layer	Surface deposition	White	25°35′32.958″N 51°29′10.053″E		
T10	13-May-2015	Sumaysimah	Dry lake bottom	Fine	Light brown	25°35′32.958″N 51°29′10.053″E		
T11	13-May-2015	Doha expressway	Surface upper layer	Grainy	Light gray	25°20′48.600″N 51°27′16.220″E		
T12	13-May-2015	Qatar University	Construction site deposits	Grainy	White	25°23′10.290″N 51°29′28.080″E		
T13	15-May-2015	Madinat Al Shamal	Surface upper layer	Grainy	Dark brown	26°06′44.744″N 51°15′22.442″E		
T14	15-May-2015	Madinat Al Shamal	Surface upper layer	Grainy	White	26°06′44.744″N 51°15′22.442″E		
T15	15-May-2015	Ain Ibn Fadl	Surface upper layer	Grainy	Red	26°03′56.333″N 51°17′53.908″E		
T16	15-May-2015	Ain Ibn Fadl	Surface upper layer	Grainy	Red	26°03′56.333″N 51°17′53.908″E		
T17	15-May-2015	Ain Ibn Fadl	Surface upper layer	Grainy	Brown	26°03′56.333″N 51°17′53.908″E		
T18	15-May-2015	Ain Ibn Fadl	Surface upper layer	Grainy	Light	26°03′56.333″N 51°17′53.908″E		
T19	15-May-2015	Ash-Shahaniyah	Surface upper layer	Grainy	White	25°25′21.420″N 51°14′14.460″E		
T20	19-May-2015	Pearl QQ beach	Beach soil deposits	Sandy with tiles black contamination	Light gray	25°22′51.096″N 51°32′52.062″E		
T21	23-May-2015	Mesaieed	Road side deposits	Hard surface crust	Light gray	24°57′45.000″N 51°31′32.200″E		
T22	23-May-2015	Sealine	Wetland deposits	Muddy crust sample	Dark gray	24°52′50.000″N 51°31′27.500″E		

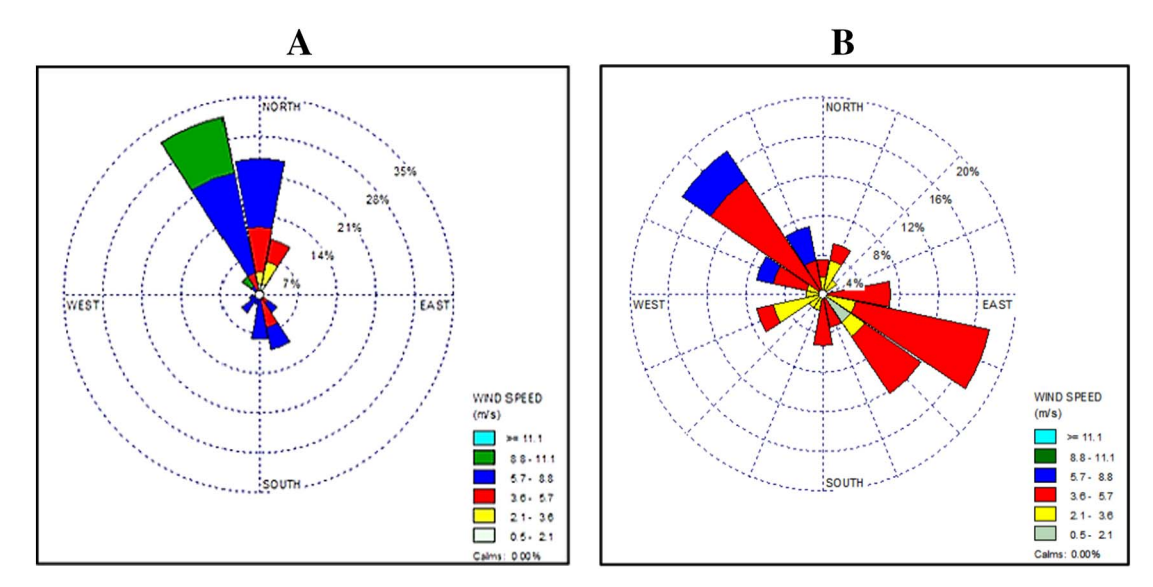


Fig. 3. Prevailing (dominant) wind direction for two consecutive days, recorded during the mega-storm sampling period on April 02–03, 2015 (A) and 18-hour of storm surge period on March 31 to April 01, 2015 (B) over the Gulf Area and the Arabian Peninsula.

of 1 month or more at most stations. When the targeted sample weight was achieved, samples were immediately collected from all stations. Sampling was mostly completed over a 48-hour period. Traps were sampled after major and super (mega) storms to collect airborne transported particles during these events. The dust particles were trapped away from wind and anthropogenic local contaminants. The last column in Table 1 shows the direction of the HYSPLIT wind trajectories for the days of the sampling intervals.

Super storm samples were collected from one of the largest historical storms ever to occur on the Qatar peninsula between the dates of April 01–02, 2015, for about 18-hour. During this massive storm, reddish dust samples were collected from permanent stations as well as indoor buildings. These were categorized separately as mega-storm dust samples, due to their unique origin and wind direction (Fig. 3). The samples were collected manually from various locations on the Qatar University campus and from three other outdoor stations using passive dust collectors (samples D10, D11, D12, D13, and D14 in Table 1).

Samples of road or traffic dust were collected during the dry, non-rainy season while driving an automobile, between the dates of April 27–June 05, 2014 (samples RD01, RD02 in Table 1). New, clean engine (for external) and cabin or passenger compartment air filters (for inside) were used for these samples. The total driving distance was 1730 km (1075 miles) inside the borders of the greater Doha metropolitan area. The filters were regularly checked to see if there was sufficient coarse particle accumulation achieved. The trapped particles were extracted from the filter tissues under vacuum in the lab, homogenized, and processed with other samples using the same acid digestion procedure.

2.2. Long-term soil/sand deposition

We also collected a representative set of surface terrestrial samples from the Qatar Peninsula. A total of 22 terrestrial deposit samples were collected from 10 different locations. Sampling information and location coordinates for these samples are given in Table 2. Sampling locations were primarily on the east coast, reflecting the long-term accumulation of both local and transported dust on top of various geological surface formations in the Qatar Peninsula. Approximately, 50 g of dry deposits were scraped from the top thin layer of dry soil, preferably from depression areas, construction sites, road sides, wet land, sand dunes, and even from a cave (Fig. 2). Care was taken to not include older (deeper) deposits. The samples were transferred to plastic vials using clean plastic spoons and double bagged in the field,

preserved at room temperature until drying and analysis.

One especially noteworthy set of samples was collected from the Musfer Sink Hole (samples T03, T04, T05, T06, T07). This medium size depression is about 100 m deep, and has the distinction of being the lowest recorded topographic point in Qatar – 53 m below sea level. This depression acts as a natural sediment trap for fine-grained atmospheric dust, located in relatively remote area, 46 km away from the center of Doha, where Al-Dafna station was located. Samples were collected from floor, walls and entrance of this deepest point of Qatar.

We also collected samples from the top and bottom of single established sand dune (samples T00, T01, T02 in Table 1), which has been in place at one site for long time. The location of this dune is labeled as Dune in Fig. 2. This dune was in southwest Qatar and stood approximately 100 m high. This a very special sampling point, because it is a well preserved, uncontaminated, very steep, and high sand dune, not preferred to be utilized by motor sports drivers. It is representative of the source materials for the atmospheric dust and terrestrial surface samples we collected. This sand dune is one of the initial dunes formed after sand particles passed the Gulf of Salva (Fig. 2) and landed over the south of the Qatar Peninsula, which is far away from the intense human activity.

3. Sample processing and analyses

Dust and terrestrial surface samples were oven dried overnight at slightly over 105 °C. Dried samples were stored in desiccators until analysis. In the laboratory, $500 \pm 50 \,\mathrm{mg}$ of homogenized samples were weighed into acid cleaned PTFE or TFM containers. Sample weight was adjusted depending on the expected concentrations of trace metals, or the amount of dust collected from the field. The samples were moistened in the acid boiled, trace metal clean Teflon tubes with about 5 ml of double distilled deionized (DDI) water, before adding a trace metal grade 1 ml HF and 12 ml aqua regia (3:1 trace metal grade mixture), composed of 9 ml HCI and 3 ml HNO3. Sample digestion was completed on a hot digestion block in a fume cupboard for the first hour at 95 °C; then continued at 135 °C during the second hour. The temperature of the hot block was adjusted carefully to prevent sample loss and to ensure total digestion. Addition of acids (HCI and HNO3) was repeated and continued until a clear digest solution was obtained. Depending on sample type, 1-3 ml of trace metal grade H₂O₂ was then added prior to evaporating the samples to complete dryness in a fume hood at 155 °C. The digest was then cooled and quantitatively transferred into a 50 ml acid cleaned volumetric glass flask which was then

made to 50 or 100 ml final volume using 2% $\rm HNO_3$ in Milli-Q deionized water, stored in dark at 4 $^\circ C$ until analysis.

A subset of atmospheric dust samples was also leached with acetic acid (HAc) and hydroxylamine hydrochloride (HyHCl) to identify the more labile concentrations. Dried samples were digested using the leaching process described in Berger et al. (2008). Comparative analyses by Berger et al. (2008) showed that this technique most effectively digested the biogenic portion, while leaving the more refractory elements intact (Rauchenberg and Twining, 2015). The leaching solution was composed of 25% HAc (pH 2) with 0.02 M HyHCl as a reducing agent. 5 ml of leachate was added to 300 mg of homogenized dry sample in a Nalgene test tube. The test tubes were placed in a beaker of water and raised to a temperature of 95 °C for 10 min, then left at room temperature for another 2 h before centrifuging at 2500 rpm for 5 min. After the leachate was removed from the sample, 5 ml of water was added to the tube and then shaken vigorously to ensure mixing. Tubes were then centrifuged at 2500 rpm for 5 min, after which the water was removed. This rinsing step was performed three times. The leach solutions were discarded and the leached solids were digested for analyses. The labile concentrations were obtained by difference in composition between unleached and leached solids.

Sample analyses were conducted by Inductively Coupled Argon Plasma Optical Emission Spectrometer (ICP-OES; Perkin-Elmer -Optima 7300 DV). Initial calibration verification (ICV 1640a) was done before the laboratory analysis to meet the criteria for laboratory analytical accuracy. Quality Control was conducted using reagent blanks, duplicate samples, spiked samples, and a certified reference material (CRM) PACS-2, collected in Esquimalt by the National Research Council of Canada (NRC) for every 10 samples. These CRM's were verified within 5% of their expected values for all elements. Internal quality control was applied by including a blank and duplicates with each analytical sample batch (typically 10 samples). The square of correlation coefficient (\mathbb{R}^2) was > 0.99 for each calibration curve, up to a concentration of 20 µg/ml. The precision was about 10%. In almost all cases the average measured values were within the 95% confidence limits of certified values, and thus the accuracy determined from this approach was comparable to or better than the precision.

A subset of samples was analyzed for mineralogy using X-ray powder diffraction (XRPD) using Cu K α radiation. Mineral phases were identified using the International Center for Diffraction Data (ICDD) data base updated to 2003.

4. Results

Elemental composition of natural-unleached dust samples are provided in Table 3. Compositions are presented in 3 categories, based on their sample type: outdoor atmospheric dust (Table 3A), mega-storm dust (Table 3B), and road dust (Table 3C). Major elements (Al, Ca, Fe, K, Mg, Na) are given as weight %, while minor and trace elements are given as parts per million (ppm). The average concentrations and standard deviations of individual elements are given at the bottom of each table and compared with average Upper Continental Crustal concentrations (UCC), using values from Rudnick and Gao (2003). The chemical composition of the UCC is an important reference material for understanding the composition and chemical differentiation of the continental crust as a whole and the Earth in general. Comparison with UCC is the generally accepted standard reference for comparing rock, soil, and dust samples to identify compositional anomalies. For example, Scheuvens et al. (2013) recommended UCC for their interpretation of the origin of Northern African dust. Concentrations that differ by more than 2σ from the averages are put in boxes. The main difference between our Qatar samples and UCC results from the calcareous nature of the Qatar samples, with a corresponding increase in Ca and Mg and decrease in other four majors (given in an order of decreasing % difference from crust): $K \ge Al > Fe > Na$ (Table 3A). Si and Ti were not analyzed in this study due to limited amount of collected dust samples. Trace element increases relative to UCC were observed for Se > Sn > Mo > Ag > Zn \ge Ni. In contrast, several trace elements were depleted relative to UCC. Negative differences were observed for Be < Ba < Mn < Pb < P < Co. Atmospheric passive dust deposition samples from Sealine, (D07, March 2015 and D19, May 2015) had unusually high values for Na (Table 3A). These elevated sodium concentrations probably originated from seawater aerosols collected at the coastal Sealine station. Enriched elemental concentrations were observed for the mega storm samples (Table 3B) and for the road dust samples (Table 3C). Comparing metal enrichments for the three types of samples showed that mega-storm dust had higher Al and Fe concentrations than the other atmospheric dust and road dust but still relatively lower concentrations than in UCC due to the very high Ca content.

The Qatari surface terrestrial samples were included in this study to compare compositional similarities and differences of these source deposits with atmospheric dust particles. The elemental composition of natural-unleached terrestrial samples in Qatar is given in Table 4 for 22 samples from 10 representative sampling sites. The blackish metallic deposits, such as the sample from single dune formation at Al Galail (sample T02), have elevated Mn concentrations and probably accumulated due to particle sorting due to wind on the top of the sand dunes. The elevated Mn suggests the particles may be coated with MnO_x as seen in desert varnish (Potter and Rossman, 1979). Higher than average metal concentrations were observed for samples T07, T09, and T20. The sample T07 was an anomalous yellowish colored sample from a layer in the Musfer sink hole wall which had 5 to 10-fold enrichments for Al, Fe, K, As, Be, Li, Mo, Pb, V, Zn and depletion for Ca, Mn, Sr, Pb relative to other surface deposits. T20 was an artificial beach sand (The Pearl Qanat-Quartier beach) with black particle contamination, where Fe, Mn, and V were enriched while Ca, Mg, Ni, Sr were pronouncedly depleted. Sample T09 was a pure crushed local surface rock or construction filling material with extremely high Ca concentration from Sumaysimah site. These three samples were mostly not included in calculations of the sample average and shown in a square in the Table 3. Average elemental concentrations and standard deviations are given at the bottom of each table for the rest of the sample set. As seen for the atmospheric dust samples (Table 3) elevated concentrations relative to UCC were observed for Ca (5 fold), but not for Fe, Al, K (~ -0.7 fold). The elemental concentrations of Qatari terrestrial surface samples had larger differences from UCC than the dust samples (except for Cd and Mo). A major increase was observed for the concentration of Ag (27 fold), followed by Cr, Sr, Mg, and, As, relative to UCC. An especially large increase (145 times larger than UCC) was observed for Ag in sample T21 which is a road site deposit from Mesaieed. The elemental concentration of many metals, categorized as anthropogenic pollutants, such as Be, Pb, P, Zn, Ba, Cu, Mn, Co, Li, and V had negative % differences (-0.9 to -0.4) relative to UCC. This was probably due to the relatively high percentage of Ca and Mg, which suggest a dilution effect due to carbonate minerals.

While average continental crust (e.g. UCC) is traditionally used for comparisons, another way of evaluating Qatari dust elemental compositions locally is to compare them with average North African (Saharan) dust. In Table 5, we compare UCC with North African dust (Moreno et al., 2006; Castillo et al., 2008), Qatari atmospheric (outdoor) dust (Table 3A) and Qatari terrestrial surface deposits (Table 4). The North African dust is noticeably more enriched in aluminosilicate (Al_2SiO_5) elements like Al, Fe, and K. The Qatari dust and surface deposits are more enriched in Ca, Mg, and Sr.

The enrichments and depletions for elemental metal concentrations of normal atmospheric (black) and mega-storm (red) dust, relative to Upper Continental Crustal (UCC) (solid line) and terrestrial surface deposits (TSD) (dashed line) from Qatar are shown in Table 3. Most of the elements are more enriched in the mega-storm samples than in the other samples. The elements Ca, Mg, Pb, and Sn have the same concentrations for both sample sets. The elements Al, Ca, Fe, K, Mg, Na

Table 3

The average concentration for 25 major, minor, and trace elements of outdoor dust, mega-storm dust, and road dust collected from Qatar, averaged over an extensive geographical range. The crustal average was determined using values from Rudnick and Gao, 2003. (UCC Avg: Upper Continental Crustal average; Std. Dev: standard deviation; % Diff. UCC: % difference from UCC, *abnormally high, odd P concentration with no clarifications, not used for average value calculation; the box was used to show noticeably deviated elemental values from the average)

Sample ID	AI	Ca	Fe	K	Mg	Na	Ag	As	Ba	Be	Cd	Со	Cr	Cu	Li	Mn	Мо	Ni	Pb	Se	Sn	Sr	٧	Zn	
(units)	(%)	(%)	(%)	(%)	(%)	(%)	(ppm)	(ppm)	(ppm)	(ppm)	(ppm)	(ppm)	(ppm)	(ppm)	(ppm)	(ppm)	(ppm)	(ppm)	(ppm)	(ppm)	(ppm)	(ppm)	(ppm)	(ppm)	(pr
D00	2.17	16.50	1.00	0.54	4.41	2.30	0.15	1.48	197	0.36	0.08	4.51	103	20.8	10.1	211	51.8	232	12.2	1.32	24.0	834	36.0	417	24
D01		15.15		0.61		2.51	0.24	1.38	184	0.34	0.08	3.80	78.8	12.7	10.0	191	27.0	124	5.81	1.39	24.1	897	30.3	349	2
D02	3.50	14.29		0.95		2.22	ND	4.46	277	0.61	0.23	10.4	81.3	101	18.5	413	4.14	70.0	17.6	3.81	25.7	683	62.0	253	7
D02	2.44	17.48				2.11	0.05	2.87	252	0.46	0.15	7.73	86.3	46.1	13.9	307	2.96	56.9	12.4	3.07	31.7	879	49.6	221	2
D03	2.72	15.53				3.06	ND	2.35	250	0.47	0.18	8.95	71.8	110	15.1	341	2.43	54.1	24.7	3.41	33.5	741	59.2	432	
D04 D05		14.31				3.23	0.16	2.83	276	0.65	0.18	10.2	84.0	100	18.4	418	2.43	62.1	21.2	2.94	40.3	703	63.1	359	
		17.46							265	0.50			75.5			331						907			
D06				0.60		2.96	0.11	3.06			0.13	8.18		46.1	13.6		2.19	51.2	12.1	3.79	28.2		54.2	252	
D07		11.50				7.36	ND	2.06	198	0.43	0.31	6.92	61.1	23.5	11.3	350	1.67	43.6	33.3	2.92	23.3	723	50.6	343	_
D08	2.51	15.44		1.05		2.34	0.23	2.42	247	0.38	0.13	6.14	74.3	43.6	11.3	277	5.82	52.1	22.0	2.55	27.3	705	42.3	289	*:
D09		16.83		0.93		1.90	ND	2.28	272	0.39	0.10	6.42	73.8	32.4	10.6	293	1.87	33.0	11.8	4.08	24.4	918	41.8	157	*
D15		17.96		0.65		1.43	ND	2.64	285	0.47	0.14	6.88	76.3	36.3	12.3	316	1.71	41.6	10.5	1.20	26.3	895	47.9	81.5	
D16	ND	ND	ND	ND	ND	ND	0.05	ND	ND	ND	ND	0.01	ND	ND	ND	ND	0.31	2.52	2.06	3.38	23.5	ND	ND	ND	
D17	3.71	13.76		0.88	3.10	4.10	ND	2.97	253	0.74	0.09	12.7	83.6	50.7	18.7	448	0.93	68.2	16.8	2.23	37.6	579	64.0	280	
D18	3.51	17.63	1.86	0.81	3.18	3.93	ND	2.77	281	0.50	0.16	9.28	77.1	47.1	18.8	367	2.76	53.5	13.8	3.64	40.6	729	57.5	161	
D19	3.08	13.99	2.55	0.71	3.29	5.05	ND	3.05	225	0.62	0.15	8.60	78.1	28.1	14.8	608	1.49	49.7	21.6	3.34	28.0	743	79.6	131	
D20	3.15	17.74	1.71	0.72	4.14	1.40	ND	2.52	301	0.47	0.18	8.22	76.3	31.9	14.5	350	1.71	45.9	10.8	3.31	27.4	884	53.3	92.4	
D25	1.80	15.3	0.88	0.27	3.00	0.30	_	ND	90.3	0.23	0.06	3.52	31.5	55.8	17.4	123	2.26	20.1	3.95	_	_	537	33.3	84.5	
D26	2.90	11.8	1.90	0.54	2.65	1.08	_	ND	232	0.44	0.15	9.50	81.9	50.4	65.8	367	ND	63.8	10.8	_	_	691	57.0	283	
D27	1.84	14.5	1.42	0.15	2.70	0.06		ND	204	0.2	ND	5.15	74.2	24.8	73.4	276	ND	53.4	7.83			877	48.9	117	
D28	1.43	13.2		0.28		0.33	_	ND	165	0.17	0.10	2.63	38.1	8.83	32.3	129	ND	22.6	2.63	_	_	885	26.6	26.9	
D29	1.93	11.5		0.37	3.04	0.56	_	ND	175	0.21	0.29	5.22	55.5	27.5	42.9	195	ND	31.8	2.97	_	_	839	34.0	63.0	
D30	2.13			0.39		0.50	_	ND	145	0.20	0.13	4.52	50.2	27.6	35.7	181	1.08	32.8	3.42	_	-	736	33.9	63.0	
D31	1.06			0.28		0.59	_	0.42	83.8	0.14	0	1.90	20.4	5.05	8.90	112	ND	18.7	1.07	_	_	713	17.1	67.7	
D31	1.31			0.44		2.64	-	3.22	66.0	0.21	0.23	4.36	34.4	12.91	11.72	223	ND	32.7	5.52	_	_	489	31.6	103	
	_						-													-	-				
D33	0.89			0.45		0.81	-	5.99	48.3	0.35	0.14	4.10	29.6	43.7	0.96	172	0.48	44.6	2.49	-	-	331	24.1	156	
D34	1.41	7.53		0.43		0.67	-	0.39	77.4	0.44	ND	3.69	35.5	33.1	16.4	170	1.11	41.0	3.69	_	-	713	28.6	130	
D35	2.03	15.8	0.85	0.72		1.61	-	-	312	0.30	-	2.52	33.1	13.9	10.0	239	0.15	25.8		-	-	907	34.8	36.0	
D36	2.30	7.32				1.29			272	0.37		1.46	15.4	3.74	6.89	127		12.3	2.10			227	17.3	9.53	. !
erage/	2.37	13.7	1.41		3.16	2.09	0.14	2.59	209	0.39	0.14	5.98	62.3	38.4	19.8	279	5.53	51.4	10.9	2.90	29.12	732	43.6	184	
d. Dev.	0.77	3.3	0.55		0.79	1.66	0.08	1.27	78	0.16	0.07	3.10	23.9	27.7	16.9	118	12.00	42.2	8.3	0.92	5.9	176	15.7	125	
C Avg.	8.15	2.57	3.92	2.21	1.50	2.43	0.05	1.5	550	3	0.1	10	35	25	20	600	1.5	20	20	0.09	2.1	350	60	71	
fference	-5.78	11.2	-2.51	-1.60	1.67	-0.34	0.09	1.09	-341	-2.61	0.04	-4.02	27.3	13.4	-0.22	-321	4.03	31.4	-9.07	2.81	27.02	382	-16.4	113	
Diff.UCC	-71	435	-64	-72	111	-14	183	72	-62	-87	42	-40	78	54	-1	-54	269	157	-45	3120	1287	109	-27	159	
- MEGA ST	rorm																								
Sample ID	Al	Ca	Fe	K	Mg	Na	Ag	As	Ва	Be	Cd	Со	Cr	Cu	Li	Mn	Мо	Ni	Pb	Se	Sn	Sr	٧	Zn	_
(units)	(%)	(%)	(%)	(%)	(%)	(%)	(ppm)	(ppm)	(ppm)	(ppm)	(ppm)	(ppm)	(ppm)	(ppm)	(ppm)	(ppm)	(ppm)	(ppm)	(ppm)	(ppm)	(ppm)	(ppm)	(ppm)	(ppm)	(
D-10	5.57	12.27		1.17	3.08	1.36	ND	4.49	280	1.11	0.24	14.3	112	27.5	25.6	592	2.34	84.8	14.3	2.12	28.6	479	83.3	161	
D-10	3.86	11.7	2.38	0.87	2.80	0.54		2.08	218	0.96	0.25	11.4	88.4	21.3	43.8	442	0.73	69.5	6.29			458	69.3	159	
D-11	3.92	14.40				1.37	ND	2.85	291	0.67	0.14	9.39	98.8	29.3	16.0	403	1.73	54.7	10.3	2.74	26.4	580	59.0	171	
D-12		13.46				1.68	ND	5.60	277	0.94	0.21	13.7	104	27.3	23.3	534	1.98	76.2	14.0	4.34	25.8	499	79.1	87.9	
D-12 D-13	5.16	13.53		1.11		1.33	ND	4.10	273	0.96	0.18	13.1	109	26.0	22.9	540	2.03	78.2	13.6	4.42	27.4	479	78.3	69.3	
D-13 D-14	4.37	14.45			3.62	1.27	ND	3.21	281	0.79	0.16	10.8	97.2	31.4	19.0	466	1.79	64.1	11.8	4.82	25.1	529	68.2	87.7	
						1.26		3.72	270			12.1	102	27.1	25.1	496	1.76			3.69		504	72.9	123	
erage	4.67	13.3	2.59	1.04	3.21		ND			0.90	0.20							71.3	11.7		26.7				
d. Dev.	0.72	1.1		0.12		0.38	_	1.26	26	0.15	0.04	1.9	9	3.4	9.8	71	0.55	10.8	3.1	1.18	1.37	44	9.0	46	
C Avg.	8.15			2.21		2.43	0.05	1.5	550	3	0.1	10	35	25	20	600	1.5	20	20	0.09	2.1	350	60	71	
fference	-3.48			-1.17		-1.17	N.A.	2.22	-280	-2.10	0.10	2.11	66.6	2.15	5.07	-104	0.26	51.3	-8.29	4	25	154	12.9	51.8	-
Diff.UCC	-43	418	-34	-53	114	-48	N.A.	148	-51	-70	97	21	190	9	25	-17	18	256	-41	4000	1170	44	21	73	
ROAD DL	JST																								
ample ID	Al	Ca	Fe	K	Mg	Na	Ag	As	Ba	Be	Cd	Co	Cr	Cu	Li (*****)	Mn	Mo	Ni	Pb	Se	Sn	Sr	V (====)	Zn	-
(units)	(%)	(%)	(%)	(%)	(%)	(%)	(ppm)	(ppm)	(ppm)	(ppm)	(ppm)	(ppm)	(ppm)	(ppm)	(ppm)	(ppm)	(ppm)	(ppm)	(ppm)	(ppm)	(ppm)	(ppm)	(ppm)	(ppm)	(
RD-1	2.18	14.5			3.33	1.77	-	-	313	0.34	-	4.55	59.3	130	11.3	260	3.12	39.7	11.3	_	15.1	723	44.0	356	
RD-2	2.26	13.2				1.57			271	0.46		4.93	68.5	194	8.09	284	11.1	40.3	8.16		13.8	583	42.3	358	
erage	2.22	13.9	1.30	0.67	3.28	1.67	_	_	292	0.40	_	4.74	63.9	162	9.67	272	7.11	40.0	9.72	_	14.5	653	43.2	357	
d. Dev.	0.06	0.9	0.01	0.01	0.07	0.14	_	_	30	0.08	_	0.27	6.5	45	2.24	17	5.65	0.5	2.20	_	0.9	99	1.2	2	
CC Avg.	8.15	2.57	3.92	2.21	1.50	2.43	0.05	1.5	550	3	0.1	10	35	25	20	600	1.5	20	20	0.09	2.1	350	60	71	
fference	-5 93	11 32	-2.62	-1 54	1 78	-0.76	N.A.	N.A.	-258	-2.60	N.A.	-5.26	28.9	137	-10.3	-328	5.61	20.0	-10.3	N.A.	12.4	303	16.0	286	
nerence	0.00	11.02			0	0.70	14.7 1.	14.7 1.	200	2.00		0.20	20.0	101	-10.3	-320	5.01	20.0	-10.5	IN.A.	12.7	303	-16.8	200	

have higher concentrations (> 10,000~ppm) in the mega-storm samples and show good agreement with terrestrial surface deposits (TSD) from Qatar. Most other elements differ little from UCC. Concentrations of Be, Sn, Pb, Ba are depleted for both types of samples relative to UCC and TSD (Table 3). One way to view the differences is to hypothesize that the Qatar samples are composed of two end-members: 1) a calcium carbonate (CaCO $_3$) fraction that is relatively depleted in most other

elements, 2) an aluminosilicate (${\rm Al}_2{\rm SiO}_5$) fraction with a composition similar to UCC.

To help understand the relationships between different elements, and which elements might be controlled by similar processes, we calculated linear correlations between the excess metal concentrations relative to UCC for various confidence limits (confidence intervals 90%, 95%, 99%, and 99.9%) using the Microsoft Excel data analysis tool

Table 4

The metal concentration (metals, heavy metals and phosphorus) of surface terrestrial deposits for 23 major, minor, and trace elements from various locations in Qatar. (UCC Avg.: Upper Continental Crustal average; % Diff: % difference from UCC; (Se and Sn was not measured; the box was used to show noticeably deviated elemental values from the average).

PPM (unita)	AI (9/)	Ca	Fe	K	Mg	Na	Ag	As (nnm)	Ba	Be	Cd	Co	Cr	Cu	Li (nnm)	Mn (nnm)	Mo	Ni (nnm)	Pb	Sr (nnm)	V (nnm)	Zn	P (nnm)
(units)	(%)	(%)	(%)	(%)	(%)	(%)	(ppm)	(ppm)	(ppm)	(ppm)	(ppm)	(ppm)	(ppm)	(ppm)	(ppm)	(ppm)	(ppm)	(ppm)	(ppm)	(ppm)	(ppm)	(ppm)	(ppm)
T00	1.48	9.59	0.32	0.78	0.63	0.94	_	_	225	0.28	_	0.96	7.3	7.69	5.75	84.1	_	7.11	_	566	10.3	5.47	87.0
T01	1.87	12.1	0.38	0.78	0.70	0.76	0.15	1.82	192	0.26	0.05	1.98	18.0	2.69	6.39	115	0.74	8.82	2.25	815	13.1	5.65	114
T02	3.21	15.9	2.74	0.57	1.24	0.90	ND	0.17	165	0.52	0.03	6.66	310	5.86	8.02	1288	1.48	18.4	6.27	926	84.2	22.8	35.9
T03	2.93	14.5	1.11	0.79	2.36	0.99	0.68	0.67	273	0.36	0.07	4.87	139	20.1	8.12	346	0.95	22.1	10.3	554	38.3	25.6	144
T04	2.93	13.8	0.93	0.86	2.43	1.10	1.32	1.49	292	0.28	0.11	4.55	79.5	12.9	8.89	250	1.24	20.9	7.35	738	32.2	19.6	197
T05	2.76	13.6	0.83	0.83	2.52	1.11	0.14	1.67	421	0.48	0.06	4.32	62.5	10.8	9.11	212	0.93	19.1	6.43	563	34.6	18.1	261
T06	3.02	11.6	0.78	0.98	1.68	1.22	0.94	2.01	237	0.34	0.10	3.74	68.3	6.13	9.18	228	0.92	16.9	6.31	479	26.1	12.4	132
T07	7.31	0.69	4.03	3.79	3.15	2.27	ND	25.5	151	2.10	0.01	6.63	124	27.3	72.56	95.3	27	66.7	16.2	142	191	55.7	66.4
T08	2.19	21.9	1.01	0.61	3.07	0.96	0.44	3.95	121	0.40	0.12	4.80	77.8	11.2	13.92	252	2.89	27.7	ND	1207	44.9	18.6	138
T09	0.72	34.9	0.16	0.28	0.48	0.66	0.29	1.40	20.5	0.04	0.12	1.57	13.2	1.61	4.77	133	1.28	3.70	ND	218	8.90	1.82	55.5
T10	2.69	21.2	1.35	0.75	2.89	0.87	2.10	2.85	224	0.22	0.23	6.70	82.5	12.1	15.62	344	1.64	38.0	5.52	556	44.8	31.3	323
T11	1.96	13.8	0.69	0.68	2.43	1.00	2.31	1.35	231	0.02	0.08	4.10	46.4	43.3	7.07	169	1.02	17.5	11.4	612	23.0	50.6	96.4
T12	1.94	16.1	0.55	0.70	2.93	0.83	2.55	1.65	289	0.28	0.05	3.02	29.2	7.89	7.47	142	0.79	12.2	2.99	1061	20.7	52.1	89.8
T13	2.69	17.4	1.50	0.73	5.45	2.06	0.08	5.22	181	0.55	0.08	8.87	91.4	15.2	19.47	380	2.20	50.9	3.38	883	46.4	27.2	327
T14	2.36	22.2	1.31	0.65	4.24	0.98	0.17	2.94	226	0.46	0.15	7.26	93.2	13.8	15.01	358	1.40	40.2	2.52	1544	38.4	28.3	354
T15	2.84	16.4	1.60	0.72	5.53	3.07	0.30	6.87	205	0.54	0.04	8.36	96.6	17.1	18.34	380	1.56	48.8	3.06	474	52.8	27.3	325
T16	3.32	15.4	1.86	0.81	5.30	2.71	0.06	5.49	216	0.65	0.05	10.1	102	19.2	20.49	435	0.80	61.2	5.01	536	56.6	37.9	380
T17	3.83	15.5	2.12	0.96	5.30	0.92	2.79	4.57	263	0.34	0.16	11.3	120	19.7	22.27	503	1.83	68.7	8.56	519	62.9	41.1	479
T18	2.74	17.6	1.52	0.77	5.33	1.98	0.79	4.39	294	0.44	0.15	8.14	94.1	15.7	16.28	402	1.73	45.9	4.06	666	46.3	30.6	364
T19	2.11	18.2	0.63	0.65	2.84	0.99	2.15	1.72	264	0.05	0.10	3.46	60.9	6.47	8.18	203	0.98	14.7	2.04	748	28.7	12.8	116
T20	1.80	4.30	4.28	0.66	0.26	0.76	0.32	ND	183	0.45	ND	5.33	92.1	3.69	4.28	1507	0.87	7.23	11.1	178	127	27.6	ND
T21	1.75	9.86	0.55	0.65	2.52	8.21	7.25	2.26	136	0.81	0.26	2.60	25.4	6.07	7.67	112	6.80	13.02	3.64	823	18.9	19.4	97.6
T22	2.58	9.07	0.61	0.97	2.24	2.70	0.93	1.55	203	0.27	0.04	2.87	35.0	5.26	8.94	170	0.94	14.28	4.11	557	19.9	18.2	121
Average	2.56	15.3	1.12	0.76	3.08	1.72	1.40	2.77	233	0.29	0.10	5.43	82.0	13.0	11.8	319	1.62	28.3	5.29	741	37.2	25.3	209
Std. Dev.	0.59	3.84	0.63	0.12	1.59	1.69	1.73	1.81	65.7	0.31	0.06	2.85	64.1	8.89	5.29	258	1.37	18.37	2.74	276	18.4	12.9	129
UCC Avg.	8.15	2.57	3.92	2.21	1.5	2.43	0.05	1.5	550	3	0.1	10	35	25	20	600	1.5	20	20	350	60	71	700
Difference	-5.59	12.7	-2.80	-1.45	1.58	-0.71	1.35	1.27	-317	-2.71	0.00	-4.57	47.0	-12.04	-8.19	-281	0.12	8.32	-14.71	391	-22.8	-45.74	-490.90
% Diff.UCC	-69	495	-71	-66	105	-29	2694	85	-58	-90	1	-46	134	-48	-41	-47	8	42	-74	112	-38	-64	-70

(similar to Yigiterhan et al., 2011). The correlation chart for all 23 elements analyzed is shown in Table 6 for Qatari atmospheric dust data. Correlation coefficients are shown for various levels of significance at P=0.100, P=0.050, P=0.010, and P=0.001. There are 3 major elements (Al, Fe, K) with which most of the elements are strongly correlated. Al is > 99.9% correlated at the significance level of P=0.001 ("r" should be larger than 0.55) with Fe (r=0.76), K (r=0.70), Ba (r=0.80), Be (r=0.83), Co (r=0.85), Cr (r=0.73), Cu (r=0.55), Mn (r=0.81), Pb (r=0.63), V (0.83) and P (0.68). Al

is > 99% but < 99.9% correlated $(0.55 \le r \ge 0.41)$ with Ca (r=0.54), Mg (r=0.51), Na (r=0.52), and Zn (r=0.43) at P=0.01 level. Similarly Al, Fe, and K are correlated with the same list of elements plus Na and Zn (for Fe) and Na, Zn, Mg, Ag, As, Cd (for K). High linear correlation coefficients (≥ 0.999) were observed between Al and Mg (except Ca), as well as Be and Cd. This suggests that most minor elements are associated with the Al₂SiO₅ fraction, not with CaCO₃. All correlations with Ca are very small, except Mg, Ba, and Sr. Scatter plots and element ratios suggest that many elements have the

Table 5

The average elemental concentration of upper continental crust (UCC) (Rudnick and Gao, 2003), North African dust (Moreno et al., 2006; Castillo et al., 2008), dust and terrestrial surface deposits from Qatar (this study). All measurements are in ppm. The percent difference is relative to UCC (Diff.: Difference; % Difference).

Element	UCC	Dust from N. Africa	Diff.	% Diff.	Dust from Qatar	Diff.	% Diff.	Deposits from Qatar	Diff.	% Diff.
Al	81,500	115,025	33,525	41	23,718	- 57,782	- 71	25,600	- 55,900	- 69
Ca	25,658	45,975	20,317	79	137,330	111,672	435	152,876	127,218	496
Fe	39,176	50,213	11,037	28	14,052	-25,124	- 64	11,193	-27,983	- 71
K	22,121	20,350	- 1771	- 8	6155	-15,966	- 72	7615	-14,506	- 66
Mg	14,955	15,000	45	0	31,606	16,651	111	30,813	15,858	106
Na	24,259	9675	- 14,584	- 60	20,871	- 3388	- 14	17,152	-7107	- 29
Ag	0	_	_	_	0.14	0	_	1.4	1	_
As	2	6	4	200	2.59	1	30	2.77	1	39
Ba	550	462	- 88	- 16	209	- 341	- 62	233	- 317	- 58
Be	3	_	_	_	0.39	- 3	- 87	0.29	- 3	- 90
Cd	0	1	1	_	0.14	0	_	0.1	0	_
Co	10	8	- 2	- 20	5.98	-4	- 40	5.43	- 5	- 46
Cr	35	211	176	503	62.3	27	78	82	47	134
Cu	25	27	2	8	38.4	13	54	13	- 12	- 48
Li	20	16	-4	-20	19.8	0	- 1	11.8	-8	- 41
Mn	600	86	- 514	- 86	279	- 321	- 54	319	- 281	- 47
Mo	2	2	0	0	5.53	4	177	1.62	0	- 19
Ni	20	27	7	35	51.4	31	157	28.3	8	42
Pb	20	36	16	80	10.9	-9	- 46	5.29	- 15	-74
Se	0	1	1	_	2.9	3	_	_	_	_
Sn	2	12	10	500	29.1	27	1355	_	_	_
Sr	350	179	- 171	- 49	732	382	109	741	391	112
V	60	89	29	48	43.6	- 16	- 27	37.2	- 23	- 38
Zn	71	75	4	6	184	113	159	25.3	- 46	- 64
P	700	2038	1338	191	415	-285	- 41	209	- 491	- 70

Table 6

The correlation/regression statistical analysis for Qatari outdoor dust samples. Linear-correlations coefficients for the mean values of 23 elements were determined at various confidence limits (for confidence intervals 90%; 95%, 99%, and 99.9%) using Excel data analysis tool. Correlation co-efficient values are shown for various levels of significances: a) underlined are significant at P = 0.100, b) a plus bolded are significant at P = 0.050, c) b plus highlighted gray color are significant at P = 0.010, d) c plus bordered are significant at P = 0.001. The linear-correlation coefficient "R" vs. the number of observations.

	Element	AI	Ca	Fe	ĸ	Mg	Na	Ag	As	Ва	Ве	Cd	Со	Cr	Cu	Li	Mn	Мо	Ni	Pb	Sr	V	Zn	Р
	Al	1.0																						
	Ca	0.5	1.0																					
	Fe	0.7	0.2	1.0																				
	к	0.7	0.2	0.4	1.0																			
	Mg	0.5	8.0	0.3	0.3	1.0																		
	Na	0.5	0.1	0.6	0.5	0.2	1.0																	
	Ag	-	-	-	0.5	0.2	0.1	1.0																
	As	0.1	-	0.3	0.2	-	0.0	0	1.0															
	Ва	<u>8.0</u>	0.6	0.4	0.7	0.5	0.3	-	0.0	1.00														
	Be	8.0	0.2	8.0	0.7	0.3	0.6	-	0.3	0.57	1.0													
	Cd	0.1	-	0.2	0.1	-	0.3	-	0.3	0.13	0.0	1.0												
	Co	<u>8.0</u>	0.4	0.9	0.5	0.4	0.5	0.1	0.3	0.54	0.8	0.2	1.0											
	Cr	0.7	0.6	0.6	0.3	0.7	0.4	-	0.0	0.58	0.5	0.0	0.7	1.00										
	Cu	0.5	0.2	0.6	0.3	0.2	0.1	-	0.4	0.30	0.5	0.1	0.7	0.43	1.00									
	Li	0.0	-	0.0	-	-	-	-	-	0.01	-	0.1	0.1	0.18	0.02	1.00								
	Mn	0.8	0.3	0.9	0.5	0.4	0.6	-	0.3	0.58	8.0	0.2	8.0	0.68	0.48	0.06	1.00							
	Мо	-	0.1	-	-	0.4	-	0.3	-	-	-		-	0.46	-	-	-	1.00						
	Ni	0.2	0.3	0.1	0.0	0.4	0.1	0.3	-	0.10	0.2	-	0.2	0.63	0.06	-	0.12	0.95	1.00					
	Pb	0.6	0.3	0.7	0.6	0.4	8.0	0.3	0.0	0.53	0.6	0.3	0.7	0.59	0.51	-	0.75	-	0.23	1.0				
	Sr	0.1	0.7	0.0	-	0.7	0.0	-	-	0.38	-	-	0.1	0.52	-	0.23	0.19	0.23	0.23	0.1	1.00			
	V	<u>0.8</u>	0.4	0.9	0.4	0.4	0.5	-	0.2	0.59	0.7	0.2	0.9	0.74	0.60	0.18	0.96	-	0.14	0.7	0.27	1.00		
	Zn	0.4	0.2	0.4	0.3	0.4	0.5	0.4	-	0.22	0.5	0.0	0.5	0.68	0.55	-	0.40	0.51	0.67	0.6	0.13	0.45	1.00	
	Р	0.6	0.2	8.0	0.5	0.2	0.6	-	0.3	0.43	0.7	0.3	8.0	0.51	0.64	0.01	0.77	-	0.07	8.0	0.03	0.77	0.55	1.00
For N		27	27	27	27	27	27	7	19	27	27	23	28	27	27	27	27	21	28	27	27	27	27	28
values→		21	21	21	21	21	21	,	19	21	21	23	20	21	21	21	21	21	20	21	21	21	21	20
P↓	r ↓																							
values	equals																							
if, P = 0.100	<u>r_</u>	0.25	1.09	0.18	0.08	0.26	0.54	0.06	0.50	25.70	0.05	0.03	1.00	7.83	9.10	5.53	38.81	4.52	13.59	2.74	57.73	5.16	41.07	67.37
if, P = 0.050	<u>-</u>	0.30	1.31	0.22	0.09	0.31	0.66	0.07	0.61	30.97	0.06	0.03	1.20	9.44	10.96	6.67	46.77	5.46	16.37	3.30	69.57	6.22	49.50	81.22
if, P = 0.010	r	0.41	1.78	0.29	0.13	0.42	0.89	0.11	0.84	41.87	0.08	0.04	1.63	12.76	14.82	9.01	63.23	7.45	22.10	4.46	94.04	8.41	66.91	109.93
if, P = 0.001	r_																				125.45	11 22	89 26	146 91
	-	0.00	2.07	3.03	5.17	3.00	,0	3.70	7	30.00	J.,,	3.00	,0	2	. 0., 7	. 2.02	57.07	. 0.00	20.70	J. U T	. 20. 10		30.20	. 70.01

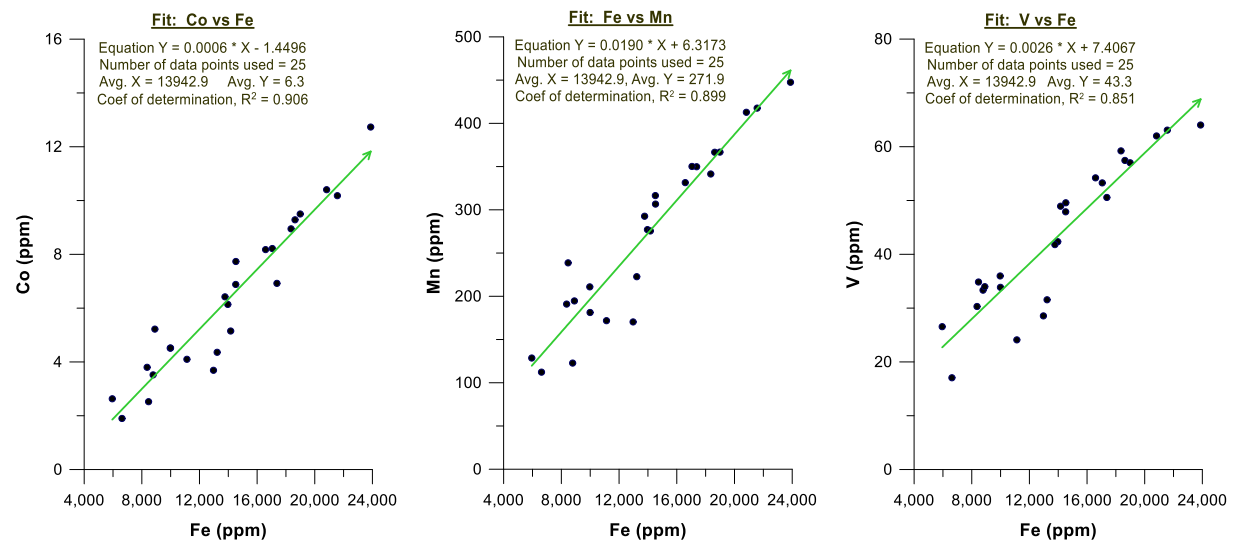


Fig. 4. Elemental concentration ratios with the three highest (Co/Fe = 0.906, Mn/Fe = 0.899, V/Fe = 0.851) positive linear correlations coefficients.

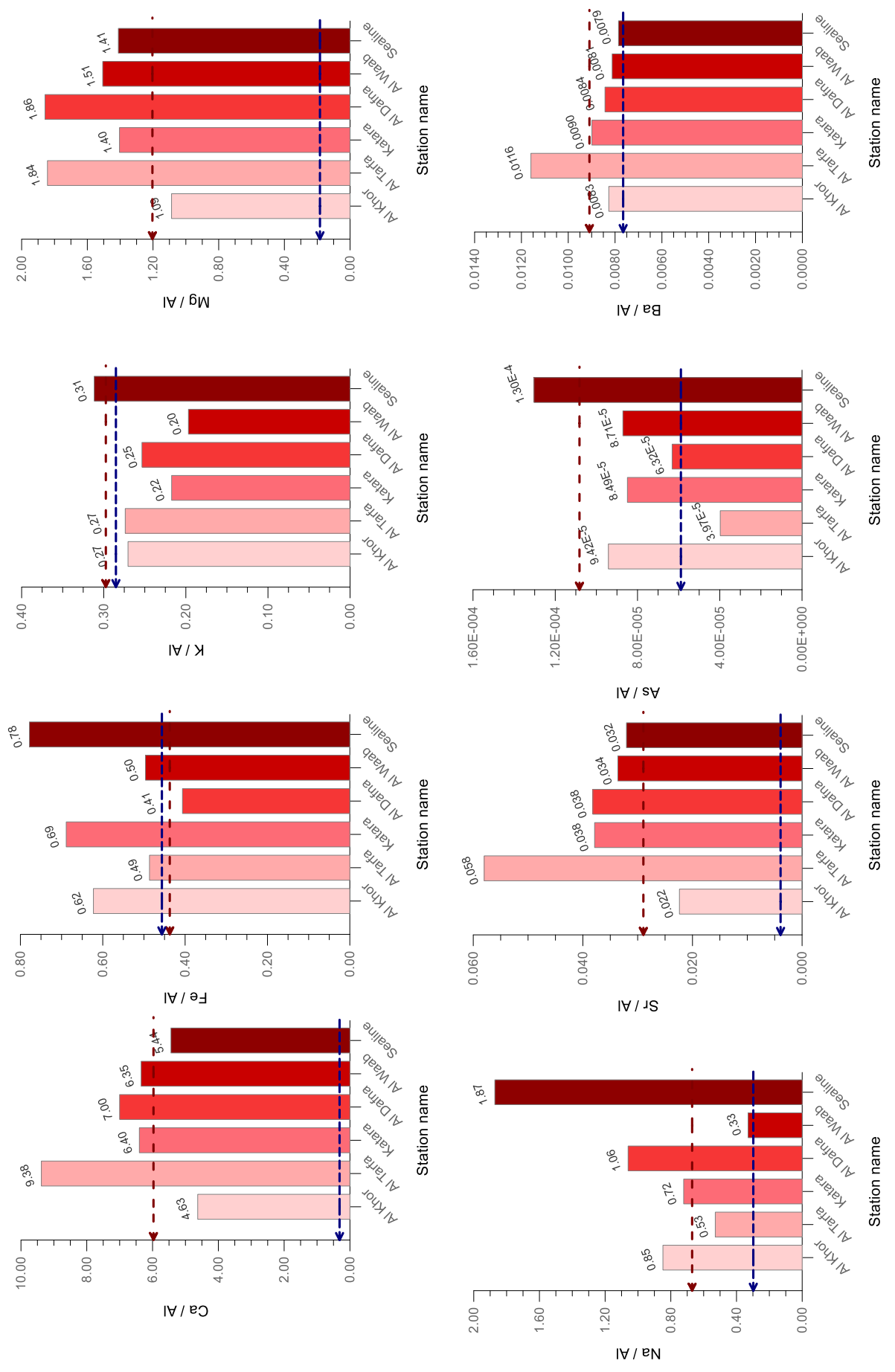
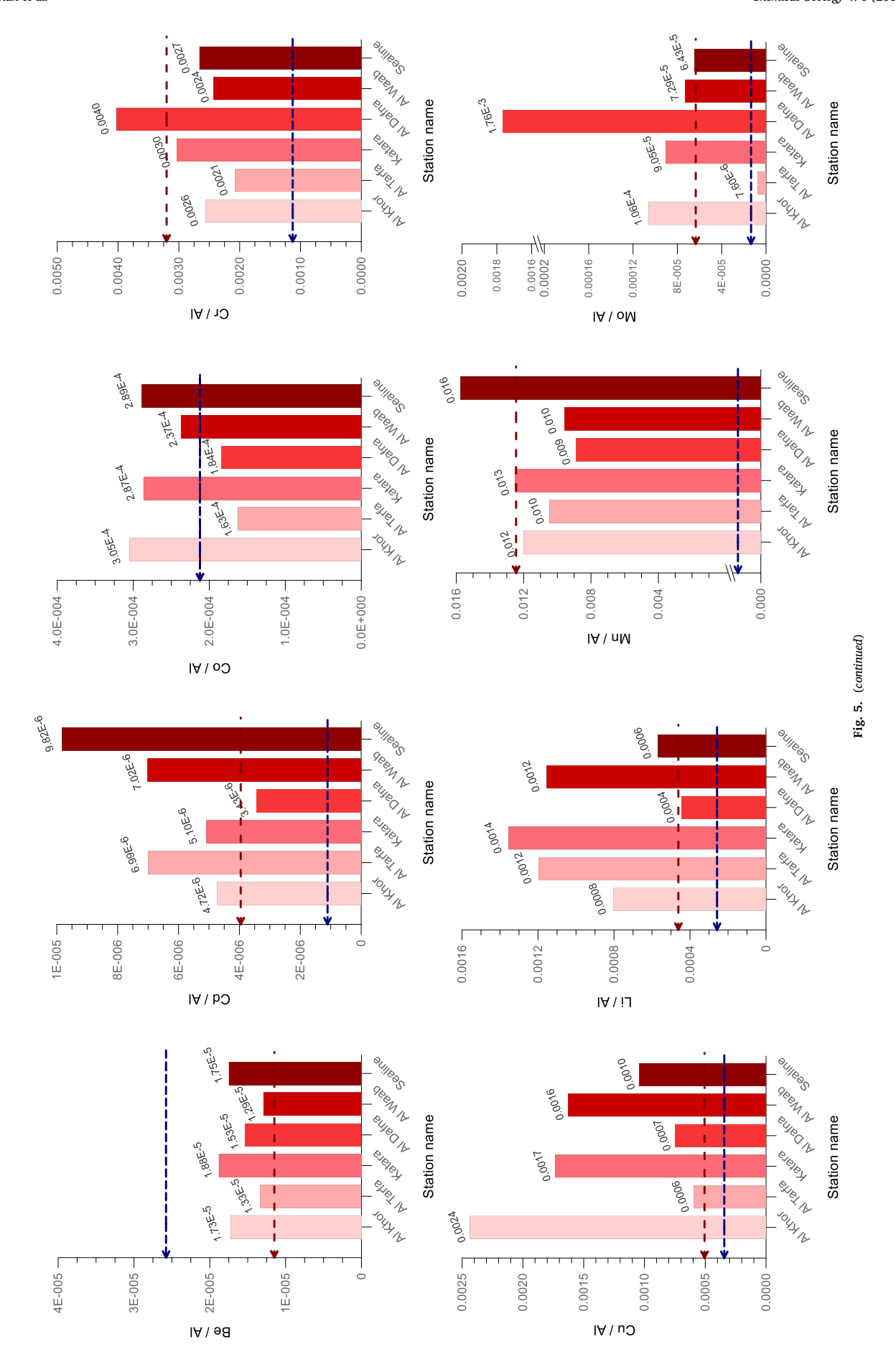
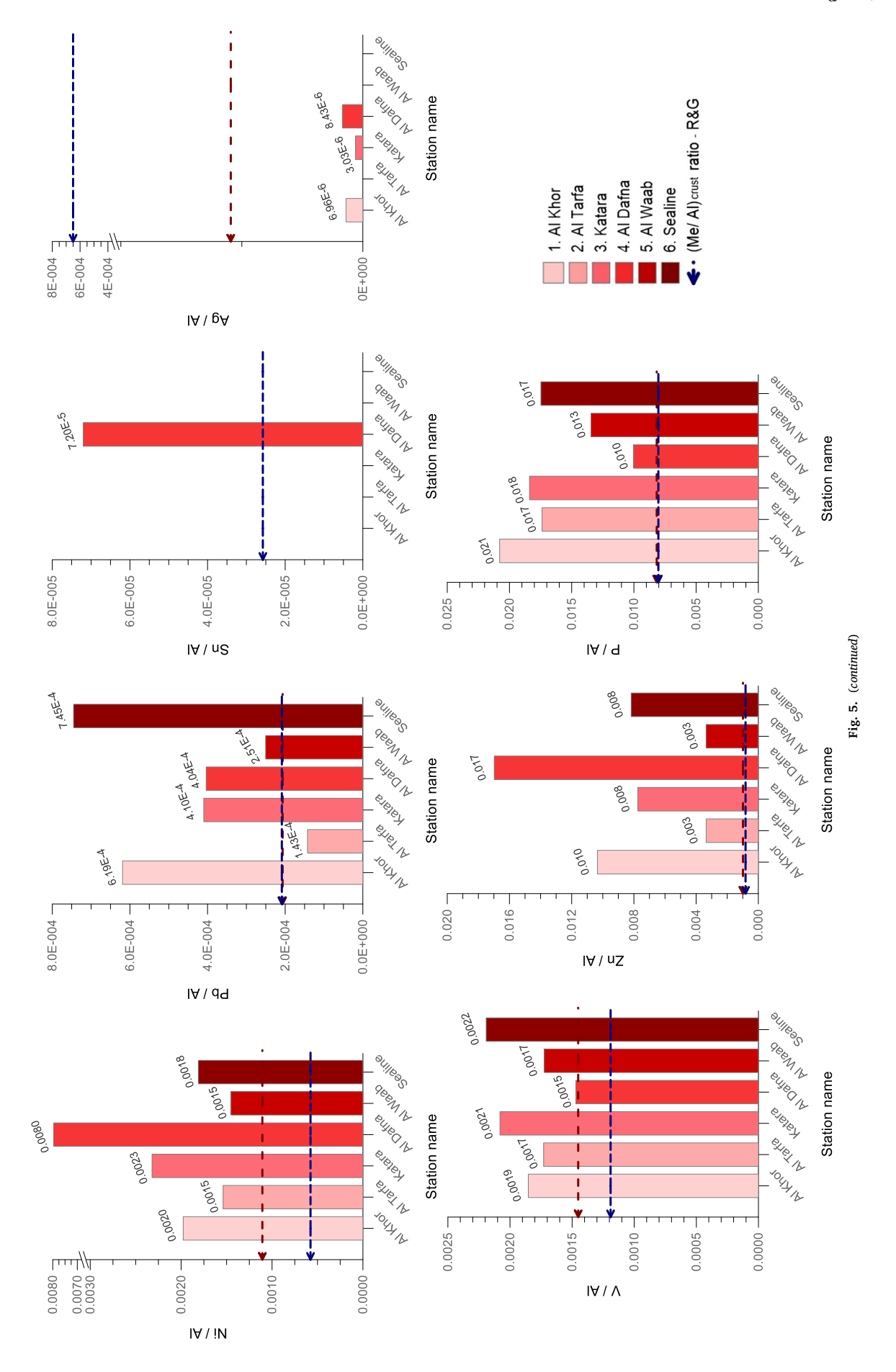


Fig. 5. Bar graph for Qatari dust samples showing mean metal to aluminum elemental ratios, based on sampling location. Linear Me/Al elemental ratios in dust samples from Qatari Peninsula are given at Y-axis and showing the enrichment relative to averages of upper continental crust (UCC) values (Rudnick and Gao, 2003) showed as horizontal dashed lines.





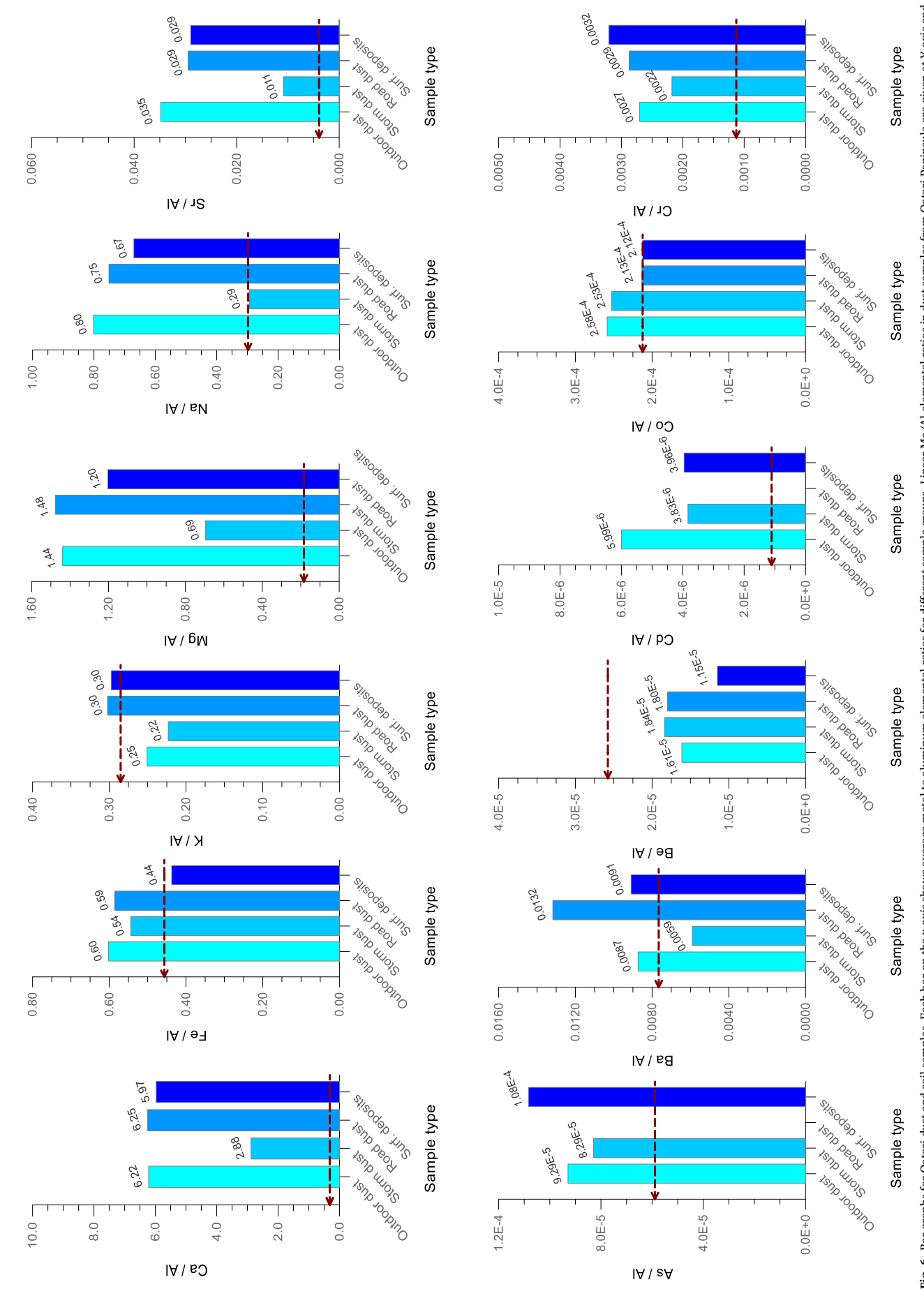
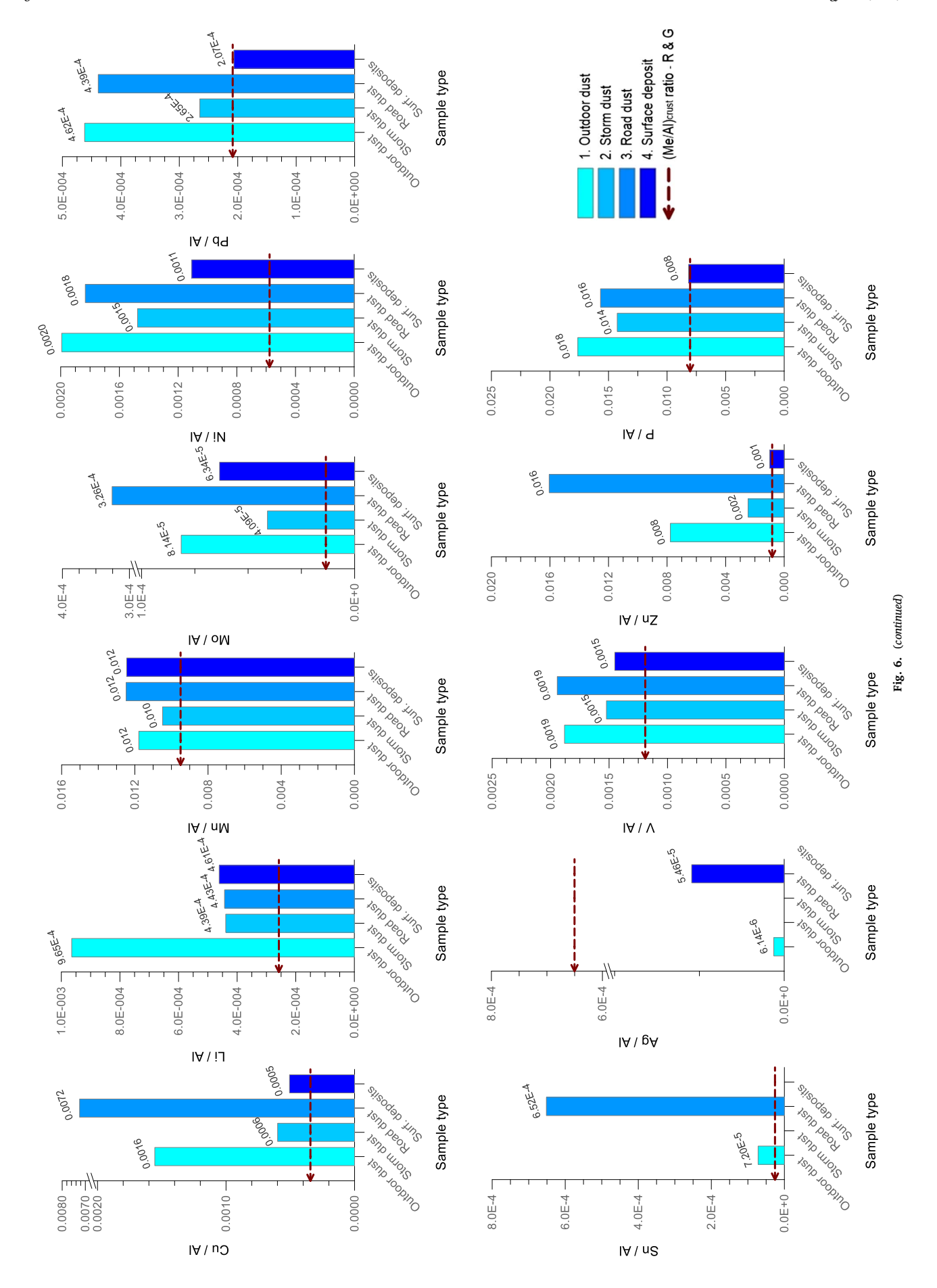


Fig. 6. Bar graphs for Qatari dust and soil samples. Each bar on the x-axis shows average metal to aluminum elemental ratios for different sample groups. Linear Me/Al elemental ratios in dust samples from Qatari Peninsula are given at Y-axis and showing the enrichment relative to averages of upper continental crust (UCC; Rudnick and Gao, 2003). The dashed lines are averages of UCC.



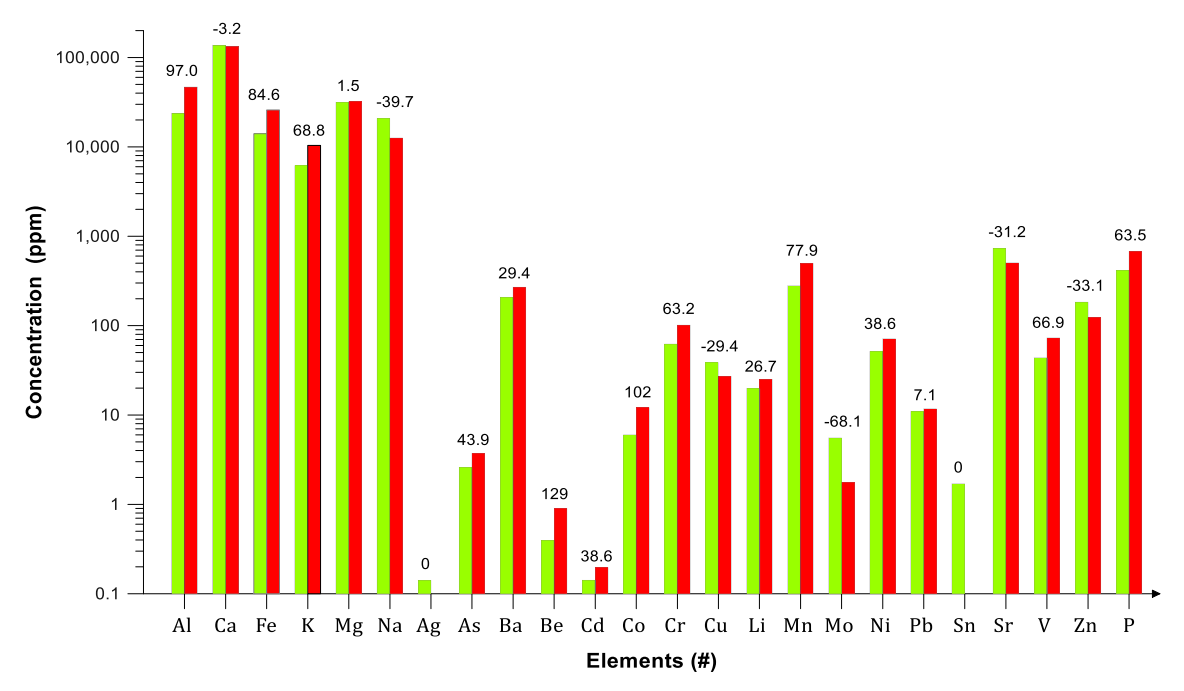


Fig. 7. The average log concentrations of elements for non-dust storm (green) and mega-dust storm (red) days. The number given at the top of each bar shows the % percentage difference as positive or negative change between non-stormy and stormy days for sampling period in Qatar.

Table 7
Shows the average of enrichment factors ± standard deviations for the major components of all kind of samples (outdoor dust (non-stormy period), mega-storm dust (stormy period), road dust (traffic dust), and terrestrial surface deposits) with respect to upper continental crust (UCC) in the study area. Note: terrestrial deposit samples T07, T09, T20 has not been used for calculating averages due to their abnormal values.

Elements	Outdoor dust	Mega-Storm dust	Road traffic dust	Terrestrial deposits
Ca	19.7 ± 5.9	9.22 ± 1.70	13.9 ± 0.9	19.68 ± 5.92
Fe	1.27 ± 0.44	1.16 ± 0.07	1.30 ± 0.01	0.86 ± 0.35
K	0.98 ± 0.33	0.82 ± 0.05	0.67 ± 0.01	1.14 ± 0.28
Mg	7.75 ± 2.17	3.80 ± 0.63	3.28 ± 0.07	6.48 ± 2.90
Na	2.86 ± 2.12	0.90 ± 0.25	1.67 ± 0.14	2.48 ± 3.22
Ag	10.1 ± 5.1	_	_	103 ± 158
As	6.71 ± 7.62	4.24 ± 0.96	_	5.78 ± 3.33
Ba	1.29 ± 0.35	0.87 ± 0.13	292 ± 30	1.40 ± 0.46
Be	0.46 ± 0.16	0.53 ± 0.08	0.4 ± 0.08	0.28 ± 0.40
Cd	5.25 ± 3.68	3.47 ± 0.92	_	3.39 ± 2.64
Co	2.11 ± 0.64	2.12 ± 0.16	4.74 ± 0.27	1.66 ± 0.65
Cr	6.17 ± 1.79	5.11 ± 0.45	63.9 ± 6.5	6.95 ± 4.42
Cu	5.3 ± 3.61	1.93 ± 0.37	162 ± 45	1.70 ± 1.39
Li	3.7 ± 3.52	2.26 ± 1.16	9.67 ± 2.24	1.86 ± 0.62
Mn	1.61 ± 0.44	1.45 ± 0.06	272 ± 17	1.59 ± 1.01
Mo	13.5 ± 30.4	2.03 ± 0.50	7.11 ± 5.65	3.75 ± 4.40
Ni	9.67 ± 7.95	6.23 ± 0.57	40 ± 0.5	4.29 ± 2.18
Pb	1.80 ± 1.17	1.01 ± 0.17	9.72 ± 2.2	0.82 ± 0.47
Se	91.3 ± 30.8	70.3 ± 23.9	_	_
Sn	40.2 ± 5.7	21.7 ± 2.7	14.5 ± 0.9	_
Sr	7.91 ± 3.05	2.57 ± 0.54	653 ± 99	7.29 ± 3.51
V	2.54 ± 0.56	2.13 ± 0.15	43.2 ± 1.2	1.90 ± 0.67
Zn	9.03 ± 5.82	3.14 ± 1.46	357 ± 2	1.16 ± 0.71
P	1.97 ± 1.10	1.70 ± 0.13	349 ± 64	0.92 ± 0.45

same source as Al, whereas relative contributions of few elements, such as Li and Al vary with concentration, suggesting different source inputs.

Elemental concentration ratios for three highest positive linear correlations coefficients (Co/Fe: 0.91, Mn/Fe: 0.90, V/Fe: 0.85) are shown in Fig. 4. This suggests that Co, Mn, and V may be originated from a similar dust source with Fe. But because Mn correlates so strongly with Fe the explanation could be due to scavenging of V and Co by either Fe or Mn oxides or both. The geochemical relationship between Co and MnO $_{\rm x}$ has been well studied and is due to oxidation of Co (II) to Co(III) by MnO $_{\rm x}$ (Murray and Dillard, 1979).

Another way to compare data in different types of samples and

sources is by calculating metal to aluminum ratios (Me/Al). This is the traditional approach because it helps to identify enrichments and depletions of reactive elements because Al is considered an immobile element and is a diagnostic tracer for lithogenic or terrigenous inputs in dust due to its high crustal abundance as Al₂O₃ (Martin et al., 1991; Yigiterhan and Murray, 2008; Yigiterhan et al., 2011). Ti may be a better choice (Ohnemus and Lam, 2010; Lam et al., 2015) but our data set did not include Ti analyses. Pitfalls of this approach were summarized by Van der Weijden (2002), who pointed out that spurious correlations can result. Because deposited dust samples can consist of materials from different origins, they may have similar or different

Table 8

Composition of representative unleached mega-storm dust samples compared with the average Upper Continental Crust (UCC) (Rudnick and Gao, 2003), and concentration difference is given as both ppm and %. The initial metal removed by the leach are also given as %. (The negative, red numbers indicate the % metal gained by the leach).

Element	Mega-storm dust average (unleached, ppm)	UCC values (ppm)	Concentration difference (ppm)	% Difference from UCC	% initial metal removed by the leach
Al	47,418	81,500	-34,082	41.8	34.3
As	3.67	4.8	-1	23.6	-31.8
Ва	285.18	624	-339	54.3	26.5
Be	0.89	2.1	-1	57.6	40.0
Ca	133,348	25,700	107,648	-419	81.3
Cd	0.19	0.09	0	-116	21.4
Co	11.82	17.3	-5	31.7	36.5
Cr	105.51	92	14	-14.7	24.6
Cu	28.4	28	0	-1.44	25.0
Fe	25,892	39,200	-13,308	33.9	25.3
K	10,751	23,200	-12,449	53.7	37.8
Li	20.8	21	0	1.16	25.6
Mg	31,674	15,000	16,674	-111	20.6
Mn	497.46	775	-278	35.8	61.0
Мо	2.03	1.1	1	-84.7	-1266
Na	13,655	24,300	-10,645	43.8	72.4
Ni	69.8	47	23	-48.4	-20
Р	684.72	655	30	-4.54	57.8
Pb	12.33	17	-5	27.5	45.7
Sr	529.39	320	209	-65.4	25.7
V	71.2	97	-26	26.6	28.7
Zn	166.4	67	99	-148	39.1

concentrations relative to UCC when the origin of the samples changes. The advantage of normalization is that real trend of chemical changes can be identified by ratio vs. ratio plots, such as enrichment and depletion of some elements because Al is an immobile element on the Earth surface in most scenarios. So, it is more meaningful to compare analytical data using metal to aluminum ratios ([Me]/[Al]) ratios, rather than metal concentrations alone (Yigiterhan and Murray, 2008).

Bar graphs for Me/Al ratios in Qatari atmospheric dust samples are given in Fig. 5 to show the variability by sample locations. Each bar on the x-axis shows clusters for mean Me/Al elemental ratios, based on sampling location from north to south direction. The location for each sampling station is given on the X-axis. Me/Al elemental ratios in dust samples are given on the Y-axis (values are labeled on top of each bar) and they are used as indicator of enrichments or depletions relative to averages of upper continental crust (UCC) and terrestrial surface deposits (TSD) from Qatar. These ratios, shown with red bars also allow us to compare Me/Al ratios for individual elements at each sampling location. The dark blue horizontal line (short dash) indicates the UCC Me/Al ratios, dark red horizontal line (longer dash) show the TSD Me/ Al ratios. Elemental enrichments can be seen for all elements except Ag, which is contrary to the abnormally high elemental concentrations of Ag found in dust and soil samples, given in Tables 3 and 4. Bar graphs for Me/Al ratios versus sample type are plotted in Fig. 6 to show variability due to sample type (rather than sampling location). Blue colored bars numbered from 1 to 4, indicate three different types of sources of atmospheric dust (#1, 2, 3), as well as terrestrial surficial deposition (#4). Me/Al ratios are compared with UCC and TSD (horizontal lines) for each individual element.

The chemical composition of atmospheric dust is necessary to clarify the likely source regions and anthropogenic elements. The average concentrations of 24 elements in passively collected atmospheric dust traps during non-dust storm (green bars, Table 3A) and

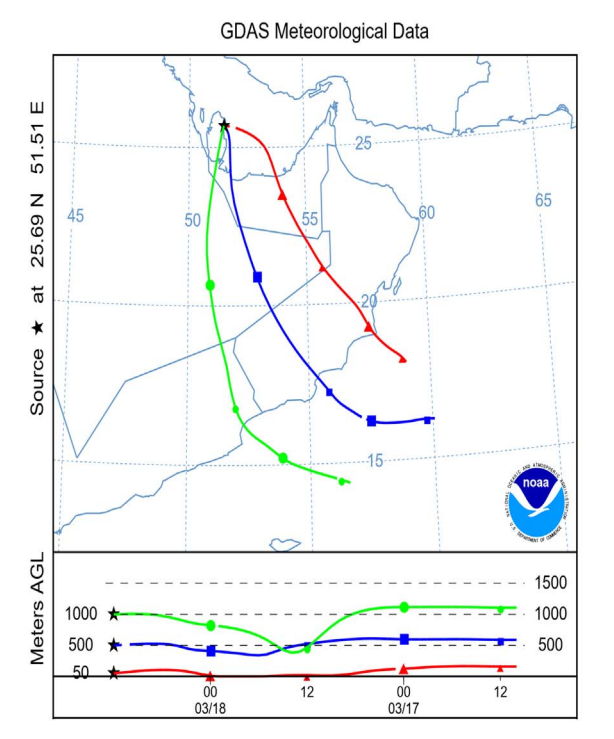
mega-dust storm (red bars, Table 3B) periods are presented in Fig. 7. The concentrations are given on a log scale. The elemental concentrations of mega-dust storms were higher than normal dust from nonstormy days for all elements except Mo > Na > Zn > Sr > Ca. The percent decrease in concentrations from non-storm to storm were Mo $(-68.1) < \text{Na} \quad (-39.7) < \text{Zn} \quad (-33.1) < \text{Sr} \quad (-31.2) < \text{Ca} \quad (-29.4)$, respectively. Both types of dust samples were equally enriched in Ca. Calcium had the maximum fraction in both non-storm $(13.7 \,\pm\, 3.3\%)$ and storm $(13.3 \,\pm\, 1.1\%)$ periods.

The concentrations of some elements increased during mega-storm days, with highest stormy/non-stormy ratios observed for Be (+129%), Co (+102%),and Al (+97%),followed bv Fe > Mn > K > V > P > Cr > As > Ni = Cd > Li > Pb between the two periods (Fig. 7). The cumulative mass of major crustal elements Al, Ca, Fe, K, Mg, and Na accounted for 23% and 26% of the total concentrations in non-dust stormy and dust stormy days, respectively (Table 3). Alghamdi et al. (2015) found that the relatively higher contribution of crustal major elements for stormy days than non-stormy days indicated that the non-local silicate rich material contributed more to dust during stormy periods than calmer periods when re-suspension of local carbonate rich dust and mixing materials containing long range transported crustal elements and other pollution species (Ho et al., 2003; Zhang et al., 2010; Liu et al., 2014).

Enrichment factors (EF) are used to reveal deviations from natural composition in soils and aerosol or to highlight differences in composition to be related to difference in origin of soils or airborne particulate matter. Enrichment factors were calculated from the general formula:

 $\mathrm{EF} = (\mathrm{Mx/Rx})/(\mathrm{Mr/Rr})$

where M is the element (metal), R is the reference element (in our case, Al), x is the sample and r is the reference sample (UCC in our case). The enrichment factors, crustal and non-crustal fractions (%) of elements



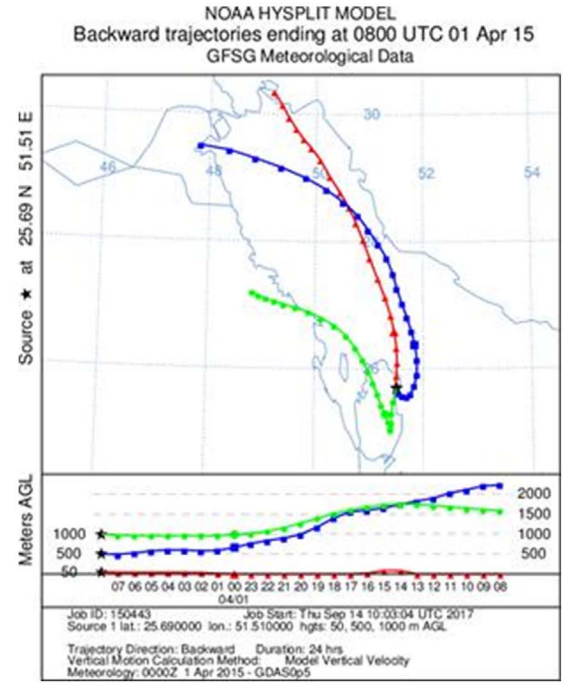


Fig. 8. Two examples of back trajectories representative of common source locations of winds blowing on Qatar. The green, blue, and red lines are isobaric contours beginning at 1000 m, 500 m, and 50 m, respectively. Each trajectory spans a 50-hour time interval, with marks every 12 h. The trajectory to the left was from 18 to 17 March 2014 (normal non-stormy date) while the one on the right was from 2 to 3 April 2015 (Mega-storm dates). These back trajectories were calculated using NOAA's HYSPLIT Trajectory Model.

relative to UCC for non-stormy (outdoor dust) and storm (mega-storm dust) and road dust are shown in Table 7. Enrichment factors (EF) were calculated with respect to two baselines: a) the average of crustal values (UCC) from Rudnick and Gao (2003) and, b) the average composition of terrestrial deposits (Table 2).

Two samples of atmospheric dust collected during the mega-storm were analyzed before and after leaching using the Berger et al. (2008) leaching procedure. The elemental concentration data for the unleached samples are shown in Table 8. The unleached data are compared with global average upper continental crust (UCC) from Rudnick and Gao (2003). Positive values for the % difference in Table 8 indicate when the concentrations of elements in these dust samples from Qatar are greater than UCC values. The leached and unleached analytical data were compared and the last column shows the % of the initial elements removed by the Berger et al. leach. The metal removed by the leach can be considered one estimate (an upper limit) of the elements solubilized when Qatari dust enters seawater. For this set of Qatari dust samples most of the Ca was removed (81%), followed by Na (72%), Mn (61%), and P (58%). Most of the rest of the elements were solubilized between 20% to 40%. Clearly the use of UCC concentrations for the lithogenic correction (as done in many studies) is not appropriate because Qatari dust has large carbonate mineral content reflecting the composition of the rocks and soils in the source regions for dust.

Semi-quantitative mineralogy results from the XRPD analyses showed that sample T2 (a representative dust sample) contained about 54% quartz, 14% calcite, 2% aragonite, 2% dolomite, and 27% assorted silicates. The total carbonate mineral content was 18%. The cave sample (T7) contained 24% quartz, 3% gypsum, and 71% assorted silicates.

5. Discussion

The deposition of Aeolian, or windblown, dust is widely recognized as an important physical and chemical flux to terrestrial and marine ecosystems. Dust deposition adds exogenous inorganic materials to ecosystems and plays an important role for biogeochemical cycling and transport of trace elements (Lawrence and Neff, 2009).

Arid environments are a major source of re-suspension of surface deposits to become atmospheric dust which supports an increase in mineral particles to remote areas. Natural resuspension is especially characteristic of arid endorheic basins such as the classic examples of the Saharan desert, and can be greatly enhanced by desertification due to human activity (Patey et al., 2015). These dusts derive from different geological and geographical sources, and the size distribution of the particles which comprise them will change with transport and time (Prospero, 1996). Transported dusts tend to be more homogeneous in particle size and composition than the fine fraction of source soils because they reflect an average of the eroded areas (Guieu et al., 2012). Bartlett (2004) stated that the Arabian Peninsula and surrounding area (Fig. 1a, b) provide multiple dust and sand source regions for different wind directions. Given the context of growing concern over the effect of desert dust resuspension on ecosystems, climate and human health, the data presented here are of interest in demonstrating the geochemical heterogeneity of such materials.

5.1. Elemental composition of Qatari dust

One of the goals of this study was to determine the composition of Qatari dust, how its composition varies at different sampling locations, and how it compares with Qatari terrestrial surface deposits. The chemical composition of atmospheric dust can be used for identifying the likely source region and provides information about trace elements of anthropogenic origin. The average concentration of 24 elements in Qatari dust is given for atmospheric dust in Table 3A, mega-storm dust in Table 3B, and for terrestrial surface deposits (including road traffic dust) in Table 3C. The compositions of these samples from Qatar reflect that they were composed of aluminosilicate and calcium carbonate materials. The Al_2SiO_5 fraction is rich in the major elements Al, Ca, Fe, Mg, K, Sr, and Na. Unfortunately, Si was not included in our data set because highly limited amount of dust was collected in each trap and these samples were analyzed by ICP-OES following total dissolution of

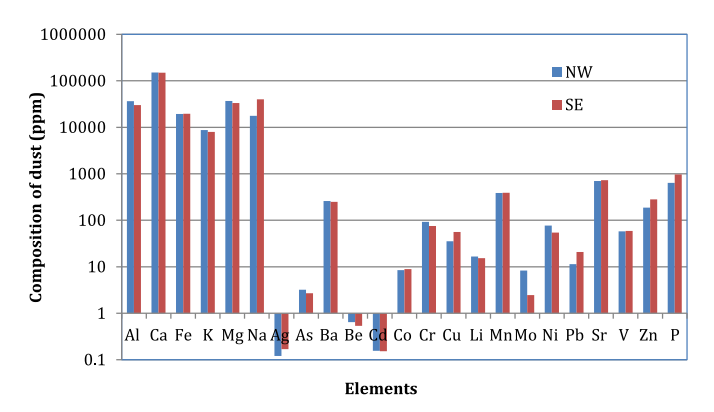


Fig. 9. Comparison of the composition of atmospheric dust from NW (blue) and SE (red) sources. The concentration scale is in ppm.

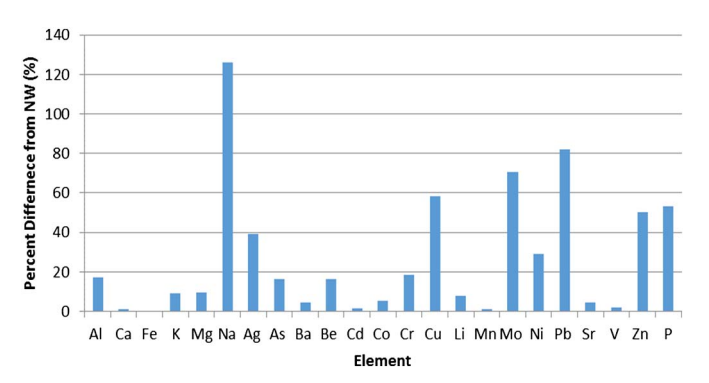


Fig. 10. The percent difference in composition of dust originating from the NW and SE directions, relative to NW composition. The elements with notable differences (> 40%) are Na, Cu, Mo, Pb, Zn, and P.

the samples using HF. However separate X-ray fluorescence (XRF) analyses showed that the SiO2 content of most of these dust samples ranged from 30% to 60%. Metal oxide coatings can enrich dust in Fe and Mn. The carbonate fraction is rich in Ca, Mg, Sr, and Li. If sea salt contributes the samples will contain the major ions of seawater, which can be traced using Na. Our samples of atmospheric dust (both background samples and mega-storm samples) and road dust are especially rich in Ca and Mg. The tracer elements for aluminosilicate material (e.g., Al, Fe, K) have lower concentrations. The ratio of Ca/Al in the Qatar background dust samples was 5.8, which is greater than the ratio in UCC of 0.32. The ratio in mega-storm dust samples was 2.8 suggesting that the carbonate fraction contributed less during these events. These are similar to the findings of Alghamdi et al. (2015), who reported the elemental composition of atmospheric aerosols during a springtime dust storm at Jeddah in Western Saudi Arabia. All three Qatari sample sets had similar sequences for major elements. In the present study, the concentrations of most aluminosilicate/metal oxide elements (especially Al, Fe, Mn) increased during stormy days suggesting that these samples may have a different source. (Table 3B; Fig. 10). Similar differences between background and storm dust were observed by Alghamdi et al. (2015).

The atmospheric dust samples were examined for their enrichment and depletion based on their sampling locations. For this, elemental ratios (Me/Al) using the atmospheric dust compositions in Table 3A, were compared at 6 different sampling locations, and the results were plotted in Fig. 5. The sequence of the station numbers are shown from north (1st) to south (6th) on the Qatar Peninsula. Al Khor was the northernmost station and Sealine was selected as the southernmost station. The Me/Al ratios, given in bar plots for 23 elements, were compared with the Me/Al ratios of crustal ratios (Rudnick and Gao, 2003) and terrestrial surface deposits (TSD) collected in Qatar for this study which are shown as horizontal lines. We observed that most

elemental ratios agreed well with the TSD line, meanwhile they were greatly enriched relative to UCC. This supports the hypothesis that most of the dust collected via passive traps is generated regionally in Qatar.

In general, the difference in composition of dust particles may vary depending on the source of those particles. For example, Aïssa et al. (2016) found that the mineralogy of Qatari dust was 58% CaCO $_3$, 34% aluminosilicate and 7% SiO $_2$. The iron in Qatar dust was most present as FeO while in iron in Saudi Arabian dust was present as clay-aggregated hematite (Fe $_2$ O $_3$). The Ca/Al ratio plot (Fig. 6) shows that Ca content, which is one of the major components for Qatari dust, can be explained by re-suspension of local deposits, rather than long distance transport to this region, since Ca/Al ratio is abnormally enriched in our samples relative to UCC ratios, but in good agreement with the mean surface deposit ratio (red dashed line).

The variability between stations (Figs. 2 and 8) also provides some clues about the possible local sources of elemental enrichments relative to UCC values. Highest Me/Al ratios for Co, Cu, and P of the 6 stations were observed at the Al Khor station (Stn. 1), this sampling location could be influenced by emissions from the industrial city of Ras Laffan when northerly winds occur. Samples from the Al Tarfa station (Stn. 2) showed high enrichments for Ca, Mg, Ba, and Sr. None of the Me/Al ratios were unusually high at the Katara station (Stn. 3), except for Be and Li. However, ratios for Fe, Co, Mn, Ni, Sr, V, P to Al give second highest peak at this station. Be is a reactive element that originates from anthropogenic activities. Li is also considered as a tracer for anthropogenic activity. Al Dafna station (Stn. 4) shows the maximum elemental ratios for Mg, Cr, Mo, Ni, Sn, Zn and enrichments for Na and Cd, which suggest contributions from car exhaust emissions and break pad dust (Grigoratos and Martini, 2014). Enrichments were also observed for many elements at Al Waab station (Stn. 5); however, concentrations were lower than the high concentrations seen at the Al Dafna station. As, Cd, and Li have the second highest enrichments at this station. The low Na/Al content suggests a smaller contribution from sea salt aerosols at Al Waab station. Strong enrichments were observed at Sealine station (Stn. 6) for the Me/Al ratios for Fe, K, Na, As, Cd, Mn, Pb and, V, which possibly reflects industrial activities, especially petrochemical and heavy metal industries. Elevated ratios were also detected for Fe, Mg, As, Co, Cu, Ni, and, P.

5.2. Comparison of Qatari dust with UCC

To show the difference between different types of samples they were categorized according to their sample type in Fig. 6. These data can be used to compare the average compositions of dust particles on a normal non-stormy day in Qatar, with a mega-storm day, with a day driving all day in heavy road traffic and with surface deposits. Average Me/Al ratios for individual samples were grouped depending on their location. These groups are: atmospheric dust (bar 1), road traffic dust (bar 2), mega-storm dust (bar 3), and local surface terrestrial deposits (bar 4) (shown from left to right). Enrichments and depletions are seen for each elemental ratio relative to crustal Me/Al ratios (see Fig. 6 legend).

Enrichments relative to UCC (Rudnick and Gao, 2003) were observed for all elements except Ag and Be. This suggests that a fraction of many elements may be associated with $CaCO_3$, which has very low (or no) Al content. K/Al values were slightly less than crustal averages. This is mainly caused by the very low Al concentrations in local dust (71% less Al than UCC) due to the dilution effect caused by the high $CaCO_3$ content. Such enrichments are not seen in other regions with high Al (e.g. Middle Eastern origin) or Fe concentrations (e.g. Saharan origin; +28.2% more Fe than UCC), which are dominated by aluminosilicate minerals rather than calcium carbonate (Table 5).

It was not surprising to see that the highest enrichments were observed for Ca/Al and Mg/Al ratios due to high $CaCO_3$ mineral content. The enrichment for Ca indicates that carbonate materials (calcite and dolomite) are important. Some Ca may originate from gypsum (CaSO₄) however gypsum is a minor component of the source rocks (e.g., Khalaf

et al., 1985). Average Ca in the atmospheric dust was 13.7%, which means that $CaCO_3$ makes up about 35% of the total mass. This is somewhat higher than suggested by the XRPD results but the latter are only semi-quantitative. We also observed that the Me/Al ratios for the major elements (Ca, Fe, K, Mg, and Sr for normal dust samples) were similar with each other and with the local surface deposits. This is consistent with the argument that the major part of the background dust was regionally generated from similar rock types in Qatar rather than an accumulation of a long-distance transport, e.g. Saudi or Kuwaiti desert dust. The Me/Al ratios for the mega-storm samples were significantly lower for Ca, K, Mg, Na, and Sr suggesting that mega-storm dust may have a different source that is richer in aluminosilicate than carbonate minerals.

The concentrations of Al and Fe were almost twice as large in megastorm dust compared with non-mega-storm dust, while Ca had slightly lower concentrations (Table 3a, b) (Fig. 7). Although Al increased by 97% in the mega-storm samples, the influence of higher Al concentration on the Me/Al ratios was limited, due to elevated mega-storm dust metal concentrations for some elements, such as Fe (84.6%), and K (68.8%) (Fig. 7). As a result, storm dust had similar Me/Al ratios for Fe and K as in the non-storm dust (Fig. 6).

It was not surprising that elemental metal concentrations for outdoor engine and passenger cabin filter samples were similar. As a result we combined the compositions of these samples to calculate the average for this study to compare with outdoor dust concentrations. Road traffic dust had almost the same Al, Ca, and Fe concentrations (Table 3c) as atmospheric dust (Table 3a). However, the Me/Al ratios for Ba, Cu, Mo, Sn, Zn, and Pb were elevated (Fig. 6, bar #3), which probably reflects anthropogenic particles generated by exhaust from internal combustion gasoline engines. It has been noted that roadside soils in other regions, near heavy car traffic, are often enriched in Pb, Cd, Cu, and Zn (e.g., Wong and Mak, 1997).

5.3. Comparison of Qatari dust with Saharan, Saudi and Kuwaiti dust

The Saharan desert and the Arabian Peninsula are the major dust storm regions in the world but the compositions of the dust can be quite variable. This makes it difficult to characterize the source regions for specific dusts.

Africa's Saharan Desert is the largest source of mineral dust in the world, covering > 3 million square miles and causing dust particles to blanket African skies (Zhao et al., 2011). This dust source represents about one half of the total global atmospheric mineral dust burden, and its uplift, transport and deposition have strong impacts on climate and various terrestrial and marine ecosystems. The chemical data set of Scheuvens et al. (2013) shows that while northern African dust is dominated by Si, there are some source regions (Morocco, Egypt, Libya) that provide carbonate minerals. The ratio of (Ca + Mg)/Fe is a useful tracer for characterizing the carbonate contribution of different source regions. For Saharan dust sources this ratio mostly ranges from 0.4 to 2.1, with a few values as high as 12.6. In Qatar, these ratios are all between values 15 to 23 (Table 3). Saharan dust generally has comparable Fe and Mn concentrations with respect to UCC and is slightly depleted in the alkali metals K and Na, and enriched in P. Depletions of Fe, Mn, P and enrichments of Na, K in Oatari dust are different from the observations of Scheuvens et al. (2013) for Saharan dust. In general, the carbonate rich Qatari dust has a different composition than aluminum-silicate rich Saharan dust.

Other, more local, source regions in Kuwait and Saudi Arabia are more likely to contribute to Qatari dust. Dust in Kuwait is mostly quartzitic calcareous silt derived from the Mesopotamian flood plain in Iraq (Khalaf et al., 1985; Al-Dousari and Al-Awadhi, 2012). Quartz is the most common mineral (75%) of the sand fraction, and calcite is the dominate mineral in the silt size fraction. Overall the gross mineralogy is mostly calcite (35%) and quartz (27%). Kukal and Saadallah (1973) found $CaCO_3$ as high as 69% in Iragi dust storms. Dust from Riyadh city in Saudi Arabia can also have high carbonate content (17% to 49%;

average of 32%) (Modiahsh, 1997; Modaihsh and Mahjoub, 2013). In western Saudi Arabia dust appears to have local sources and consist of a combination of carbonate and aluminosilicate minerals (Alghamdi et al., 2015). A little further away, in the Gulf of Aqaba in the northern Red Sea, the mineralogy of dust, inferred from chemical composition, is silicate rich (3.5% dolomite, 15% calcite, 21% Al-silicate and 51% quartz) (Torfstein et al., 2017).

5.4. Comparison of dust with terrestrial surface deposits and cave deposits

We compared the composition atmospheric dust in Oatar with various terrestrial surface deposits and samples of dust deposited in caves. Most of Oatar's area is flat, low-lying desert, which rises from the east to a central limestone plateau reflecting a broad geological anticline along the axis. Soils in Qatar contain small amounts of organic material and are generally calcareous and agriculturally unproductive. Windblown sand dunes are common (especially in the south), and soil distribution over bedrock is light and uneven. Soil salinity is high in coastal regions and in agricultural regions where poor regulation of irrigation has led to increased salinity (Ann and Anthony, 2016). There are five main types of soil in Qatar. These are: rawdha soils, sabkha soils, lithosol or rocky soils, sandy soils, and man-made soils associated with cultivated areas which are a mixture of types and treatments. The soils most commonly found in Qatar are the lithosol. They are relatively thin (typically 10 to 30 cm deep) and are a calcareous sandy loam, covered with lightly weathered rock debris, overlying a layer of rock fragments over limestone bedrock (Babiker, 1990). In addition, there are approximately two thousand depressions spread around the country which contain colluvial soils made up of calcareous loam, sandy loam, and sandy clay loams to depths of between 30 cm to 150 cm (FAO, 2008). Generally, these soils are known as rawdha and are the main source for the agriculture of the country. The rawdha soils are characterized by small amounts of organic matter, low water retention properties and poor structural properties. This gives rise to surface crusting which interferes with the plant-air-water relationship and inhibits the emergence of seedlings. Sabkha soils are found in broad, flat areas near the sea, and are composed of areas of saline sand or silt, lying just above the water table and generally deposited over a long period of time by the action of wind-blown sand deposited into coastal regions. Their flatness is controlled by the humidity associated with the presence of the relatively high water table which, is typically about half a meter below the surface (West and Al-Mulla, 2013).

In this study, samples were collected from various land surface locations that reflect different proportions of rawdha, sabkha, lithosol, and sandy soils. The elemental concentrations of these soil samples were normalized to aluminum then compared with UCC and local atmospheric dust samples based on differences observed at different sampling locations. Me/Al ratios for surface soil deposits are compared with atmospheric dust and UCC ratios in Fig. 6. The comparison shows that Qatari terrestrial surface samples have very similar Me/Al ratios as Qatari atmospheric dust for most elements. Similarities were also observed with road dust for some elements. The elemental ratios for Fe, K, Co, Pb and, P are about the same as UCC. These five elements don't show any enrichment or depletions relative to crustal ratios. The largest enrichments were observed for Ca, Mg and Sr, and others (Na, As, Ba, Cd, Cr, Cu, Li, Mn, Mo, Ni, V, Zn) while depletions were only recorded for Ag and Be.

There are larger scale surficial geological features called as duhul (sinkholes) in Qatar. They are representative of the three karstic features in the country: sinkholes, simple depressions, and complex depressions. Over a period of time, a combination of groundwater and limited rainwater have reacted with these relatively soft surface and sub-surface rock formations, dissolving gypsum and limestone to form a karst system with sinkholes (karst funnels) which are found throughout Qatar. A karst system is mainly associated with gypsum-based materials but it is also influenced by carbonate rocks (Kretschmer and Jäntschke,

2012). Gypsum is occasionally present.

We collected five samples (T03, T04, T05, T06, T07) from inside and outside the Musfer sinkhole. Although these samples were carefully collected from different layers in the cave in order to represent various geochemical formations from surrounding soil in the depression area to the deepest part of the cave, they were compositionally very similar to each other (except sample T07 which contained mostly silicate minerals). This should be due to accumulated and well-mixed outdoor and storm dust mixture inside the cave where it acts like a giant dust trap and gives us perfect homogenized elemental composition in the geographical center of Qatar (largest depression area of the country). It was also observed that the average composition for samples T03 to T06 were very similar to average Oatari surface soil composition (Table 4).

Sample T09 (Sealine) has a very different composition from the rest of the samples. It has low trace metal concentrations with relatively high Ca concentrations. Later, we realized that this was an unknown surface deposit, probably introduced to region from outside Qatar by tidal waves, for construction or other purposes. Samples T07 and T09 were not used for calculating average and standard deviations (Table 4).

5.5. The comparison of dust from northern and southern sources

The winds transporting dust in Qatar come from a variety of locations, but mostly coming either from the northwest from northern Saudi Arabia and Iraq or from the southeast from Oman. The average wind directions for the last 5 years are shown in Fig. 1. We examined the composition of Qatari dust to see if there was a compositional difference that depended on the source.

Back trajectories, calculated with the NOAA program HYSPLIT, are a common way to study the transport of aerosol from source regions to receptor sites and interpretation of how aerosol or other atmospheric components vary over space and time (Alghamdi et al., 2015). The main idea behind the back trajectories is that there exists a link between air mass path and the aerosol observations at the receptor site, which is Qatar Peninsula. The back trajectories are shown for three initial elevations (1000 m, 500 m, and 50 m). The wind rose plot during the mega-dust storm occurred on April 01'st 2015, showed that the prevailing direction of wind during this 18 hour period was dominantly from the SE (Fig. 3B). Thus, the atmospheric dust must have originated form that direction. This was consistent with the back trajectories aerosol path determined for the same period. Two representative HYSPLIT back trajectories for our samples in 2015 are shown in Fig. 8. The source of air on 17-18 March 2015 was from the southeast (part of samples D01, D08, and D09) and that for 2-3 April 2015 (the date of the mega-storm) was from the northwest (samples D10 to D14).

During our initial sampling periods in 2014 dust trajectories calculated using HYSPLIT come from both the north and south and we examined the compositions of dust from these regions to determine if they had different compositions (Fig. 9). We separately averaged the twenty-one samples with northern and southern origins. These showed that the source of the dust particles was equally divided between northerly (n = 12; northern Saudi Arabia, Kuwait or Iraq) and southerly (n = 8; SE Saudi Arabia, United Arab Emirates, and Oman) sources. One sample (D04 and D06) appeared to originate from the west (Saudi Arabia). The percent differences in composition of dust originating from the NW and SE, relative to NW composition are shown in Fig. 10. For most elements, the concentrations from the SE were higher. However, only three elements had a statistically significant difference. The elements with notable differences (> 40%) were Na, Cu, Mo, Pb, Zn, and, P. There were only three elements for which there was a statistical difference between the NW and SE samples according to a t-test: Cr, Na, and Pb. Pb and Na were higher in the samples from the south while Cr was higher in those from the north. Due to the large differences between the averages, we were surprised not to find Mo on that list. However, it appears that the only reason Mo was so much higher in the NW samples was due to the first two samples (D00 and D01) taken at Al Dafna. Because the values fluctuated so much, there was no statistically distinct difference between NW and SE samples and we can't identify the source of the samples based on composition.

5.6. The leachable fraction of the dust

The compositions of two samples of Qatari dust from a mega-storm solubilized by the leaching process were compared in Table 8. The elements removed by the acid leach gives an indication of the reactive components. From the % of elements leached in Table 8, we see that many elements are leached away. Ca was efficiently removed by the leach, probably due to carbonate mineral dissolution. Na was removed and some of that may be due to sea salt aerosols as well as sodium in carbonate minerals.

One objective of conducting the acid leaches was to get an indication of what fraction of the elements may be solubilized when the dust enters seawater. The leach gives an upper limit. The actual amounts solubilized are more difficult to assess. For example, if, and how much, of the carbonate minerals will dissolve in surface seawater will depend on the state of saturation. At present that is poorly known because there has not been the necessary research done on the carbonate system parameters (e.g. dissolved inorganic carbon and alkalinity). A limited early study (Brewer and Dyrssen, 1985) suggested that the surface seawaters are saturated with respect to calcite. If that is the case the CaCO₃ would not dissolve. But in the years since that study ocean acidification has probably made the surface seawater more corrosive so the state of saturation may have changed (Doney et al., 2012).

Iron (Fe) is another element that is important as it has been argued that the input of iron associated with atmospheric dust can influence biological food-web structure and stimulate primary productivity. In our study, 25% of the Fe in dust was solubilized by the leach. The flux of phosphorus solubilized from dust (58%) is also significant.

Because river input is so small, this solubilized fraction of nutrients and metals must be a major source of bioactive elements to the surface seawater. Future studies should be conducted where samples of dust are added to surface seawater and measurements of dissolved Fe conducted before and after.

5.7. Enrichment factors

Enrichment factors (EF) can give insights into differentiating anthropogenic from natural sources (Alghamdi et al., 2015). Aluminum was chosen as the standard reference element in enrichment studies because of its abundance and because it is a crustal marker. It is supposed not to be influenced by anthropogenic factors and so it represents well the uncontaminated baseline. It has been widely used as reference in many studies regarding aerosols (Schutz and Rahn, 1982; Abrahim and Parker, 2008; Rushdi et al., 2013; Shelley et al., 2015). Rushdi et al. (2013) used enrichment factors to study atmospheric dust composition and contamination in Riyadh, Saudi Arabia. They were able to distinguish anthropogenic contamination for S and Ni, primarily from fossil fuel combustion.

Enrichment factors of about unity indicate that the dominant source of the element is crustal, while values higher than 10 may indicate either a strong difference of natural composition with respect to the chosen baseline, or an anthropogenic influence. In our case, we can observe the following trends in the EF relative to UCC (Table 7):

- The EF for Ca, Mg, Sr are correlated, while Ca and Na are not correlated, in the terrestrial surface deposits, dust and mega-storm dust samples. For Ca, Mg, and Sr this is due to the large contribution of carbonate minerals relative to Al-silicate minerals, which dominate in UCC. The lack of correlation for Na suggests that it has a different origin, probably marine aerosols.
- Mega-storm dust samples had a lower EF than background dust deposits for Ca. The average EF for Ca in mega-dust was 9.2 compared with 19.7 in background dust (Table 7). The EF for Mg and Sr

in background dust and surface deposits are also comparable. Earlier we showed that background dust had a similar composition and Me/Al ratios to local terrestrial surface deposits. These results suggest that background dust has a local origin. Because the mega-storm samples have such a lower EF for Ca (Mg, Sr, and Na), suggests that they have, at least partially, a different origin.

- In terrestrial surface deposits, the correlation between Ca/Mg and Ca/Sr is less strong, also Ca and Na are not correlated.
- For the trace metals, the main result is the strong difference between road samples, with EFs ranging from 50 to several hundreds, and dust, terrestrial surface deposits, and mega-storm samples, where EF are usually below or around 10. Se and Sn are the exception and have EF between the values of 50 to 100.
- EF for trace metals are higher than in background dust and megastorm dust. Both have higher EF than EF in terrestrial surface deposits. This suggests that background dust, which has a mineral component similar to terrestrial surface samples, are enriched by heavy metals from the local atmosphere, either by traffic or industrial emissions.
- The EF calculated for terrestrial surface deposits shows that megastorm samples are different from all the other samples and that trace metals in dust and traffic deposits samples are more enriched than in storm samples. In particular, contamination of terrestrial surface samples is the same than in traffic samples, i.e. Cu, Mo, Ni, and Zn, revealing that they might derive from the same local anthropogenic source of pollution (either traffic or industrial emissions).

6. Conclusions

The major source of atmospheric dust in Qatar is most likely local surface deposits on the Qatar peninsula. Qatar dust and local terrestrial surface deposits have similar compositions and both are enriched in carbonate, rather than aluminosilicate minerals. Oatari dust is enriched in Ca. followed by Al, Mg, and Na. The compositions differ from mean crustal values, which have much higher Al. This means that the major fraction of atmospheric dust is generated over and around Qatar, where sedimentary rocks are rich in Ca (most likely carbonate minerals, CaCO3, with some dolomite, CaMg(CO₃)₂ and minor amounts of gypsum, CaSO₄). The composition of Qatari dust differs from Saharan, Saudi and Kuwaiti dust with its higher Ca and lower Al - Fe concentrations. Kuwaiti and Saudi dust, in particular, can be highly enriched in Si (quartz). While Qatari dust is enriched with high Ca/Al and Mg/Al ratios, some depletions were observed for minor and trace constituents relative to Upper Continental Crust values. This is probably because carbonate material has lower concentrations of trace elements than the aluminosilicate (Al₂SiO₅) fraction.

Our study showed that the composition of mega-storm dust was different from background dust and terrestrial surface deposits. Background dust and mega-storm dust have different average Enrichment Factors (EF) for the major elements Ca, Mg, and Na. The EF for Ca averages 19.7 in background dust and decreases to 9.2 in mega-storm dust. This suggests that dust in the mega-storms comes from farther away, possibly northern Saudi Arabia or Kuwait.

The enrichment factors show that road dust is more enriched in heavy metals (e.g., Ba, Cu, Mo, Ni, Pb, Sn, V, and Zn) than background dust, while the major components are similar. This suggests that the origin of road dust is local (major components = crustal component) but that heavy metals are enhanced due to anthropogenic emissions from either traffic or industrial sources. Future research should study the size fractionation of particle concentrations as fine fraction of particulate dust tends to be richer in anthropogenic heavy metals than coarser fractions.

An acid leach procedure solubilized a significant fraction of almost all elements. Ca was the element most affected as the leach (81% removed) would remove any carbonate minerals present. Bioactive elements like Fe (25%) and P (58%) were also significantly solubilized. Because river input is so small to the Arabian Gulf, this solubilized fraction of dust is likely a major source of nutrients to surface seawater.

The relationship between nutrient input from dust and biological production and food-web structure should be investigated.

In this study, we included analyses of terrestrial surface deposits from various locations around Qatar in order to trace if the local deposits are source or sink for trace elements. Most of the elemental concentrations, originated from terrestrial surface deposits were similar to Qatari dust, except abnormally high Ag concentrations in some deposits. Very high elemental concentrations were observed at road dust for Sn, Cu, Zn, Mo, with enrichment factors of several hundred for Ba, Cu, Mn, Se, Zn, P, suggesting that traffic around Doha can be a source for high metal concentrations.

Acknowledgement

This is a joint interdisciplinary research reflecting the contribution of various groups of researchers. This study was mainly funded by Qatar University - Environmental Sciences Center (internally funded). The research was partially supported by QNRF-NPRP grant. The authors would like to thank Qatar National Research Fund (QNRF) for funding and supporting this project under the National Priorities Research Program (NPRP) award number NPRP# 6-1457-1-272. The manuscripts contents are solely the responsibility of the authors and do not necessarily represent the official views of Qatar National Research Fund. The statements and conclusions made herein are solely the responsibility of the authors and do not necessarily represent the official views of Qatar University, Qatar Ministry of Environment, and Qatar National Research Fund. The technical support of Ms. Hajer Ammar J A Alnaimi, Mr. Hamood Abdulla Al-Saadi, Mrs. Marwa Moustafa Al-Azhary and Mr. Mehmet Demirel from Environmental Science Center (ESC), Qatar University during field sampling, samples preparations, pretreatment, and analysis is highly acknowledged.

Appendix A. Supplementary data

Supplementary data to this article can be found online at https://doi.org/10.1016/j.chemgeo.2017.10.030.

References

Abrahim, G.M.S., Parker, R.J., 2008. Assessment of heavy metal enrichment factors and the degree of contamination in marine sediments from Tamaki Estuary, Auckland, New Zealand. Environ. Monit. Assess. 136, 227–238. http://dx.doi.org/10.1007/s10661-007-9678-2.

Aïssa, B., Isaifan, R.J., Madhavan, V.E., Abdallah, A.A., 2016. Structural and physical properties of the dust particles in Qatar and their influence on the PV panel performance. Sci Rep 6http://dx.doi.org/10.1038/srep31467. (Article number: 31467).

Al-Dousari, A., Al-Awadhi, J., 2012. Dust fallout in northern Kuwait, major sources and characteristics. Kuwait J. Sci. 39, 171–187.

Alghamdi, M.A., Almazroui, M., Shamy, M., Redal, M.A., Alkhalaf, A.K., Hussein, M.A., Khoder, M.I., 2015. Characterization and elemental composition of atmospheric aerosol loads during springtime dust storm in western Saudi Arabia. Aerosol Air Qual. Res. 15 (440–453), 2015. http://dx.doi.org/10.4209/aaqr.2014.06.0110.

Al-Naimi, H.A., Al-Ghouti, M.A., İsmail Al-Shaikh, M.A., Saeed, M.A.-Y., Al-Meer, S., 2015. Metal distribution in marine sediment along the Doha Bay, Qatar. Environ. Monit. Assess. 187, 130.

Al-Sanad, H.A., Ismael, N.F., Nayfeh, A.J., 1993. Geotechnical properties of dune sands in Kuwait. Eng. Geol. 34, 45–52.

Al-Senafi, F., Anis, A., 2015. Shamals and climate variability in the northern Arabian/
Persian Gulf from 1973 to 2012. Int. J. Climatol. http://dx.doi.org/10.1002/joc.

Ann, J., Anthony, C.J.D., 2016. Qatar, Encyclopedia Britannica Online. Retrieved 20 June, 2016, Written by Jill Ann and Crystal John Duke Anthony. http://global. britannica.com/place/Oatar.

Aumont, O., Bopp, L., Schulz, M., 2008. What does temporal variability in aeolian dust deposition contribute to sea-surface iron and chlorophyll distributions? Geophys. Res. Lett. 35, L07607. http://dx.doi.org/10.1029/2007GL031131.

Babiker, A.A., 1990. The Vegetation of the State of Qatar as Related to Landform and Soil. http://hdl.handle.net/10576/8409.

Bartlett, K.S., 2004. Dust Storm Forecasting for Al Udeid AB, Qatar: An Empirical Analysis. PhD thesis by Kevin S. Bartlett, Captain, USAF AFIT/GM/ENP-04-01 Department of the Air Force, Air University, Air force institute of Technology. In: Wright-Patterson Air Force Base. Approved for Public Release; Distribution Unlimited, Ohio.

Berger, C.J.M., Lippiatt, S.M., Lawrence, M.G., Bruland, K.W., 2008. Application of a

- chemical leach technique for estimating labile particulate aluminum, iron, and manganese in the Columbia River plume and coastal waters off Oregon and Washington. J. Geophys. Res. 113, C00B01. http://dx.doi.org/10.1029/
- Blank, M., Leinen, M., Prospero, J.M., 1985. Major Asian Aeolian inputs indicated by the mineralogy of aerosols and sediments in the western North Pacific. Nature 314, 84–87.
- Brewer, P.G., Dyrssen, D., 1985. Chemical oceanography of the Persian Gulf. Prog. Oceanogr. 14, 41–55.
- Buck, C.S., Landing, W.M., Resing, J., 2013. Pacific Ocean aerosols: deposition and solubility of iron, aluminum and other trace elements. Mar. Chem. 157, 117–130.
- Castillo, S., Moreno, T., Querol, X., Alastuey, A., Cuevas, E., Herrmann, L., Mounkaila, M., Gibbons, W., 2008. Trace element variation in size-fractionated African desert dusts. J. Arid Environ. 72, 1034–1045.
- Cavelier, C., 1970. Geological Description of the Qatar Peninsula (Arabian Gulf). Department of Petroleum Affairs, Qatar, B.R.G.M., France (39 pp).
- Chen, Y., Paytan, A., Chase, Z., Measures, C., Beck, A.J., Sanudo-Wilhelmy, S.A., Post, A.F., 2008. Sources and fluxes of atmospheric trace elements to the Gulf of Aqaba Red Sea. J. Geophys. Res. 113. http://dx.doi.org/10.1029/2007JD009110.
- Doney, S.C., Ruckelshaus, M., Duffy, J.E., Barry, J.P., Chan, F., others, nine, 2012. Climate change impacts on marine ecosystems. Annu. Rev. Mar. Sci. 4, 11–17.
- El-Baz, F., Makharita, R.M., 2009. The Gulf War and the Environment. Gordon and Breach Publishers, pp. 31–54 (178. ISBN 2-88124-649-4. ISBN 978-2-88449-100-6. Retrieved 2009-06-03).
- El-Sayed, A.E., Girgis, B.R., Rajab, M.H., Nassar, E.S., 2010. In: Trace metal concentrations in street dust samples in Zagazig City, Egypt and their risk assessment. Proceeding of Fifth Scientific Environmental Conference, 2010, Zagazig Uni. pp. 37–47.
- ESC, 2014. Geology of Qatar: A Brief Introduction. Publication of the Environmental Studies Center. pp. 2014 Qatar University, scientific content by: Fahil N. Sadooni, Ph.D, (Professor of Petroleum Geology).
- FAO, 2008. Food and Drug Administration of United Nations, AQUASTAT Survey 2008: irrigation in the Middle East region in figures. In: Frenken, Karen (Ed.), FAO Water Reports, 34. FAO Land and Water Division, Rome, pp. 2009.
- Fung, I.Y., Meyn, S.K., Tegen, I., Doney, S.C., John, J.G., Bishop, J.K.B., 2000. Iron supply and demand in the upper ocean. Glob. Biogeochem. Cycles 14, 281–295. http://dx. doi.org/10.1029/1999. GB900059.
- Guieu, C., Bozec, Y., Blain, S., Ridame, C., Sarthou, G., Leblond, N., 2002. Impact of high Saharan dust inputs on dissolved iron concentrations in the Mediterranean Sea. Geophys. Res. Lett. 29http://dx.doi.org/10.1029/2001GL014454. ISSN: 0094-8276.
- Guieu, C., Loÿe-Pilot, M.-D., Benyahya, L., Dufour, A., 2010. Spatial variability of atmospheric fluxes of metals (Al, Fe, Cd, Zn and Pb) and phosphorus over the whole Mediterranean from a one-year monitoring experiment: Biogeochemical implications. Mar. Chem. 120 (Issues 1–4), 164–178. http://dx.doi.org/10.1016/j.marchem.2009. 02.004. (20 June 2010).
- Grigoratos, T., Martini, G., 2014. Scientific and Technical Research Reports Science Areas: Energy and transport. Publications Office of the European Union ISBN: 978-92-79-38303-8 (print),978-92-79-38302-1 (pdf) ISSN:1018-5593 (print),1831-9424 (online) DOI: 10.2790/22000 (print) 10.2790/21481 (online)Other Identifiers: EUR 26648 OPOCE LD-NA-26648-EN-C (print),LD-NA-26648-EN-N (online). http:// publications.jrc.ec.europa.eu/repository/bitstream/JRC89231/jrc89231-online %20final%20version%202.pdf.
- Hanson, A.K., Tindale, N.W., Aİdel-Moati, M.A., 2001. An Equatorial Pacific rain event: influence on the distribution of iron and hydrogen peroxide in surface waters. Mar. Chem. 75 (1), 69–88. http://dx.doi.org/10.1016/S0304-4203(01)00027-5.
- Ho, K.F., Lee, S.C., Chow, J.C., Watson, J.G., 2003. Characterization of PM10 and PM2.5 source profiles for fugitive dust in Hong Kong. Atmos. Environ. 37, 1023–1032.
- Jickells, T.D., et al., 2005. Global iron connections between desert dust, ocean biogeochemistry and climate. Science 308, 67–71.
- Johansen, A.M., Hoffmann, M.R., 2003. Chemical characterization of ambient aerosol collected during the northeast monsoon season over the Arabian Sea: labile-Fe(II) and other trace metals. J. Geophys. Res. 108 (D14), 4408. http://dx.doi.org/10.1029/ 2002.ID003280.
- Khalaf, F.I., Al-Kadi, A., Al-Saleh, S., 1985. Mineralogical composition and potential sources of dust fallout deposits in Kuwait, northern Arabian Gulf. Sediment. Geol. 42, 255–278.
- Kretschmer, M., Jäntschke, M., 2012. The Doha metro tunneling in special dimensions. Tunnel 5, 34.
- Kukal, Z., Saadallah, A., 1973. Aeolian admixtures in the sediments of the Northern Persian Gulf. In: Purser, B.H. (Ed.), The Persian Gulf. Springer Verlag, Berlin, pp. 115–123.
- Lawrence, C.R., Neff, J.C., 2009. The contemporary physical and chemical flux of Aeolian dust: a synthesis of direct measurements of dust deposition. Chem. Geol. 267, 46–63.
- Lam, P.J., Ohnemus, D.C., Auroa, M.E., 2015. Size-fractionated major particle composition and concentrations from the US GEOTRACES North Atlantic Zonal Transect. In: Deep Sea Research Part II: Topical Studies in Oceanography. 116. pp. 303–320. http://dx.doi.org/10.1016/j.dsr2.2014.11.020.
- Liu, Q., Liu, Y., Yin, J., Zhang, M., Zhang, T., 2014. Chemical characteristics and source apportionment of PM10 during Asian dust storm and non-dust storm days in Beijing. Atmos. Environ. 91, 85–94.
- Martin, J.M., Windom, H.L., 1991. Present and future roles of ocean margins in regulating marine biogeochemical cycles of trace elements. In: Mantoura, R.F.C., Martin, J.M., Wollast, R (Eds.), Ocean Margin Processes in Global Change. JohnWiley & Sons Ltd.
- Martin, J., et al., 1994. Testing the iron hypothesis in the equatorial Pacific. Nature 371, 123–129.
- McGee, D., Marcantonio, F., lynch-Stieglitz, J., 2007. Deglacial changes in dust flux in the

- eastern equatorial Pacific. Earth Planet. Sci. Lett. 257, 215-230.
- Modaihsh, A.S., Mahjoub, M.O., 2013. Falling dust characteristics in Riyadh City, Saudi Arabia during winter months. APCBEE Procedia 5, 50–58.
- Modiahsh, A.S., 1997. Characteristics and composition of the falling dust sediments on Riyadh city, Saudi Arabia. J. Arid Environ. 36, 211–223.
- Moore, J.K., Braucher, O., 2008. Sedimentary and mineral dust sources of dissolved iron to the world ocean. Biogeosciences 5, 631–656.
- Moreno, T., Querol, X., Castillo, S., Alastuey, A., Cuevas, E., Herrman, L., Mounkaila, M., Elvira, J., Gibbons, W., 2006. Geochemical variations in Aeolian mineral particles from the Sahara-Sahel Dust Corridor. Chemosphere 65, 261–270. http://dx.doi.org/ 10.1016/j.chemosphere.2006.02.052.
- Murray, J.W., Dillard, J.G., 1979. The oxidation of cobalt(II) adsorbed on manganese dioxide. Geochim. Cosmochim. Acta 43, 781–787.
- Ohnemus, D.C., Lam, P.J., 2010. Cycling of lithogenic marine particles in the US GEOTRACES North Atlantic transect. Deep Sea Res., Part II 116, 283–302.
- Patey, M.D., Achterberg, E.P., Rijkenberg, M.J., Pearce, R., 2015. Aerosol time-series measurements over the tropical Northeast Atlantic Ocean: dust sources, elemental composition and mineralogy. Mar. Chem. 174, 103–119.
- Pease, P.P., Tchakerian, V.P., Tindale, N.W., 1998. Aerosols over the Arabian Sea: geochemistry and source areas for aeolian desert dust. J. Arid Environ. 39, 477–496 Article No. ae970368.
- Potter, R.M., Rossman, G.R., 1979. The manganese- and iron-oxide mineralogy of desert varnish. Chem. Geol. 25, 79–94.
- Prospero, J.M., 1996. Saharan dust transport over the North Atlantic Ocean and Mediterranean: an overview. In: Guerzoni, S., Chester, R. (Eds.), The Impact of Desert Dust across the Mediterranean. Kluwer Academic Publishers, pp. 133–151.
- Ranville, M.A., Cutter, G.A., Buck, C.S., Landing, W.M., Cutter, L.S., Resing, J.A., Flegel, A.R., 2010. Aeolian contamination of Se and Ag in the North Pacific from Asian fossil fuel combustion. Environ. Sci. Technol. 44, 1587–1593.
- Rauchenberg, S., Twining, B.S., 2015. Evaluation of approaches to estimate biogenic particulate trace metals in the ocean. Mar. Chem. 171, 67–77.
- Rudnick, R.L., Gao, S., 2003. Composition of the continental crust. In: Rudnick, R.L. (Ed.), The Crust. vol. 3. Elsevier, pp. 1–64.
- Rushdi, A.I., Al-Mutlaq, K.F., Al-Otaibi, M., et al., 2013. Air quality and elemental enrichment factors of aerosol particulate matter in Riyadh City, Saudi Arabia. Arab. J. Geosci. 6, 585–599. http://dx.doi.org/10.1007/s12517-011-0357-9.
- Samhan, O., Zarba, M., Anderlini, V., 1986. Aeolian contributions of trace metals to marine sediments of Kuwait. Environ. Int. 12 (6), 611–617.
- Scheuvens, D., Schütz, L., Kandler, K., Ebert, M., Weinbruch, S., 2013. Bulk composition of northern African dust and its source sediments—a compilation. Earth Sci. Rev. 116, 170–194.
- Schutz, L., Rahn, K.A., 1982. Trace-element concentrations in erodible soils. Atmos. Environ. 16 (1). 171–176.
- Shelley, R.U., Morton, P.L., Landing, W.M., 2015. Elemental ratios and enrichment factors in aerosols from the US-GEOTRACES North Atlantic transects. Deep-Sea Res. II 2015. http://dx.doi.org/10.1016/j.dsr2.2014.12.005i.
- Siefert, R.L., Johansen, A.M., Hoffmann, M.R., 1999. Chemical characterization of ambient aerosol collected during the southwest monsoon and intermonsoon seasons over the Arabian Sea: labile-Fe (II) and other trace metals. J. Geophys. Res.-Atmos. 104 (D3), 3511–3526.
- Sur, S., Owens, J.D., Soreghan, G.S., Lyons, T.W., Raiswell, R., Heavens, N.G., Mahowald, N.W., 2015. Extreme aeolian delivery of reactive iron to late Paleozoic icehouse seas. Geology 43, 1099–1102.
- Torfstein, A., Teutsch, N., Torosh, O., Shaked, Y., Rivlin, T., Zipori, A., Stein, M., Lazar, B., Erel, Y., 2017. Chemical characterization of atmospheric dust from a weekly time series in the north Red Sea between 2006 and 2010. Geochim. Cosmochim. Acta 211, 373–393.
- Van der Weijden, C.H., 2002. Pitfalls of normalization of marine geochemical data using a common divisor. Mar. Geol. 184, 167–187.
- Wang, R., Balkanski, Y., Boucher, O., Bopp, L., Chappell, A., Ciais, P., Haughustaine, D., Penuelas, J., Tao, S., 2015. Sources, transport and deposition of iron in the global atmosphere. Atmos. Chem. Phys. 15, 6247–6270.
- West, I., Al-Mulla, M.M., 2013. Qatar Geology, Sabkha, Evaporates and Desert Environments. Internet Webpage. http://www.southampton.ac.uk/~imw/Qatar-Sabkhas.htm Version: 20th January 2013.
- Windom, H., 1975. Eolian contributions to marine sediments. J. Sediment. Petrol. 45, 520–529.
- Wong, J.W.C., Mak, N.K., 1997. Heavy metal pollution in children playgrounds in Hong Kong and its health implications. Environ. Technol. 18 (1), 109–115.
- Yigiterhan, O., Murray, J.W., 2008. Trace metal composition of particulate matter of the Danube River and Turkish rivers draining into the Black Sea. Mar. Chem. 111 (1–2), 63–76
- Yigiterhan, O., Murray, J.W., Tugrul, S., 2011. Trace metal composition of suspended particulate matter in the water column of the Black Sea. Mar. Chem. 126 (1–4), 207–228 20 September 2011.
- Yigiterhan, O., Turner, J., Al-Ansari, E.M.A.S., Abdel-Moati, M.A.R., Paul, B., Nelson, A., Al-Yafei Al-Ansi, M.A.A.A., Murray, J.W., 2017. Trace Element Composition of Plankton from the Qatari EEZ of the Arabian Gulf. in submission.
- Zhang, W., Zhuang, G., Huang, K., Li, J., Zhang, R., Wang, Q., Sun, Y., Fu, J.S., Chen, Y., Xu, D., Wang, W., 2010. Mixing and transformation of Asian dust with pollution in the two dust storms over the northern China in 2006. Atmos. Environ. 44, 3394–3403.
- Zhao, C., Liu, X., Leung, L.R., Hagos, S., 2011. Radiative impact of mineral dust on monsoon precipitation variability over West Africa. Atmos. Chem. Phys. 11 (5), 1879–1893. http://dx.doi.org/10.5194/acp-11-1879-2011.